Recent Advances in Medical Image Segmentation and Classification

László Szilágyi

Obuda University, Budapest, Hungary

Sapientia University of Transylvania, Romania

Why detect brain tumor?

- 100k++ people die of brain tumor yearly
- Early detection helps the survival

- More and more medical imaging devices
- Not so many more human experts
- Need for reliable automated algorithm
  - Draw attention to suspicious cases
  - Human expert has the last word

- Classical machine learning
- Convolutional neural networks and deep learning

Input Data

- Medical Image Computation and Computer Aided Interventions (MICCAI)
- Brain Tumor Segmentation Challenge (BraTS) since 2012
- BraTS train dataset 2019
  - 76 low-grade (LG) and 259 high-grade (HG) volumes
- Multispectral (T1, T2, T1C, FLAIR)
- 155 x 240 x 240 image volxels
- Ground truth (negative, active tumor, necrotic tumor, tumor core, edema)

- iSeg-2017 challenge: T1, T2, and GT
- No tumor, just tissue segmentation

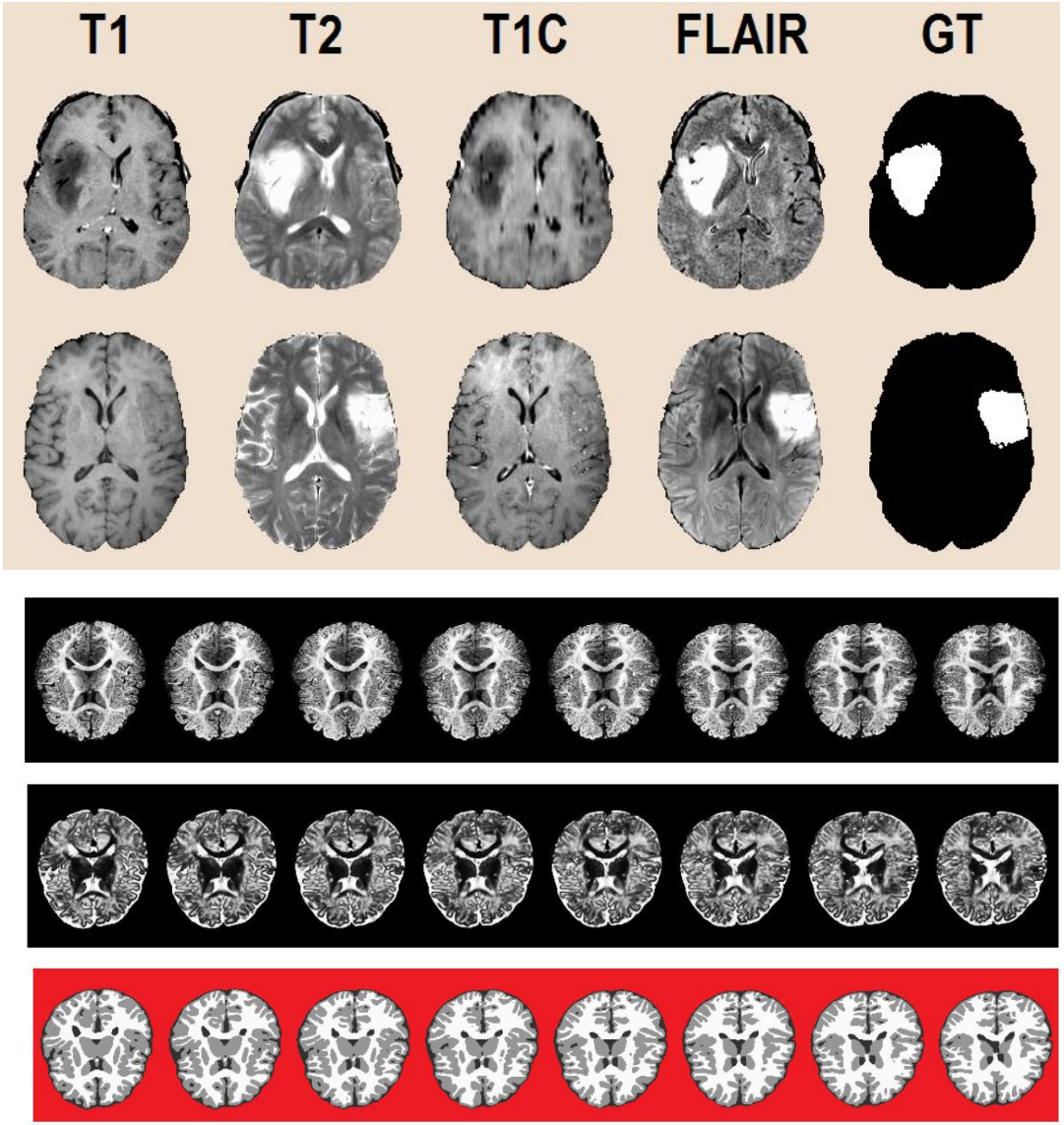

Difficulties

- Tumors have various locations, sizes, shapes, appearances
- Normal tissues are deformed, shifted
- Data channel registration is not perfect
- No standard scale of intensities
- Presence of noise, e.g. intensity non-uniformity

Solutions

- Pre-BraTS era
  - Mostly unsupervised, image-processing methods (Gordillo 2013)
- BraTS era, 1st stage, classical machine learning methods
  - Classification of individual brain pixels, lots of features extracted after serious preprocessing, post-processing to improve coherence of decisions
- BraTS era, 2nd stage, CNN + deep learning
  - CNN architectures, no hand-crafted features, less pre-processing
  - Processing whole volumes, results may need regularization
- Our focus:
  - Contribute to both chapters
  - Optimize some supportive elements of segmentation techniques
  - Data enhancement (pre-processing)
  - Extra services (during segmentation or post-processing)

No standard intensity scale

- Histograms need normalization
- Existing methods
  - Nyúl et al (2000) – piece-wise linear transform
  - Leung et al (2010) – segmentation, tissue-based alignment
  - Weisenfeld et al (2004) – Kullback-Leibler divergence
  - Shinohara et al (2011) – PCA
  - Jäger et al (2006) – hidden Markov random field
  - Linear transform

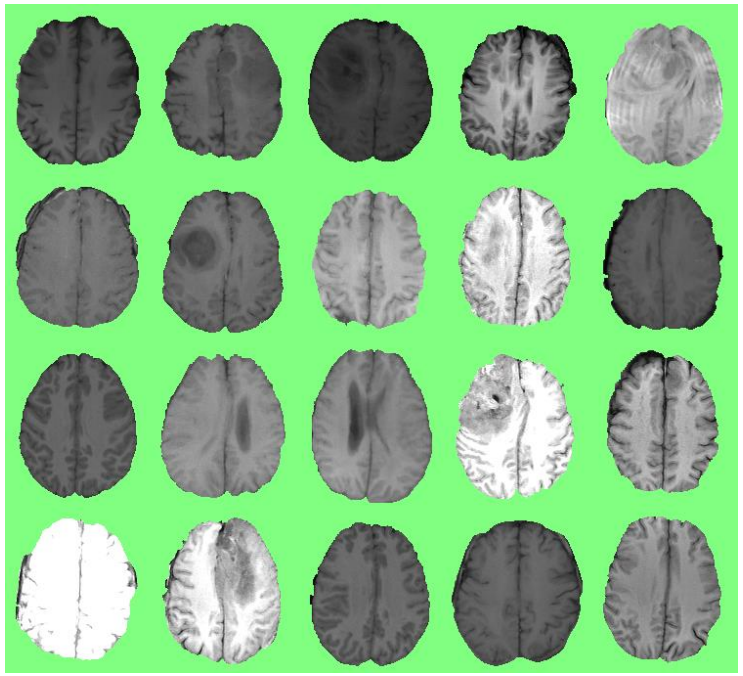

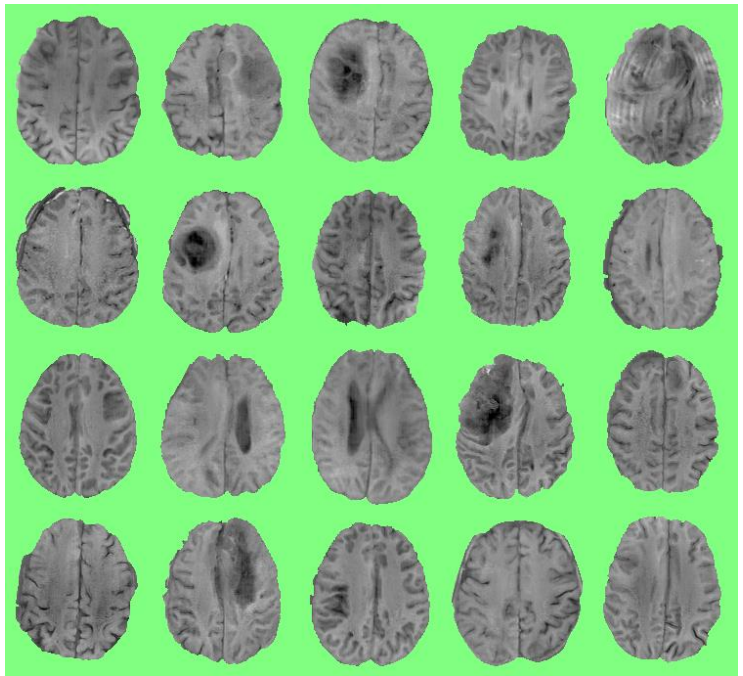

Linear vs. piece-wise linear transform

- Linear

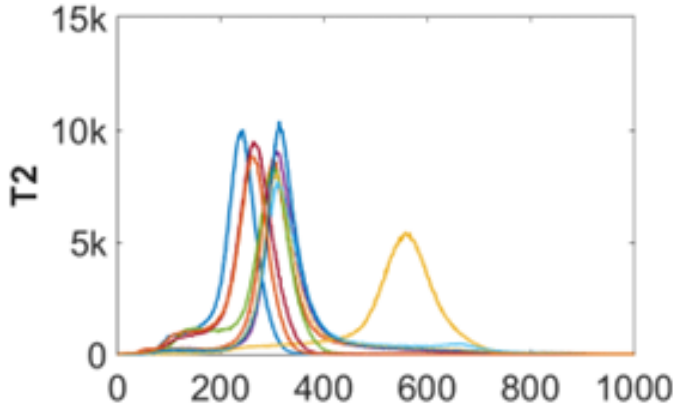

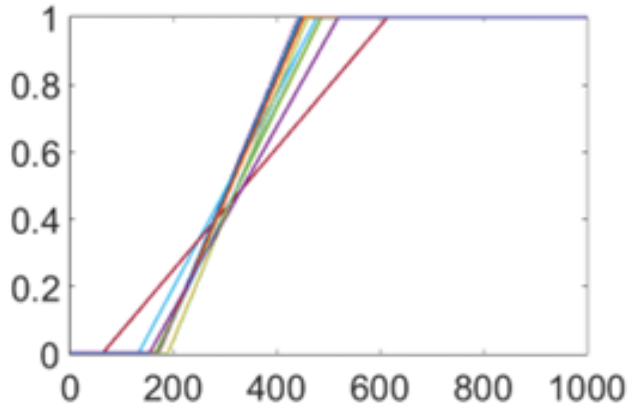

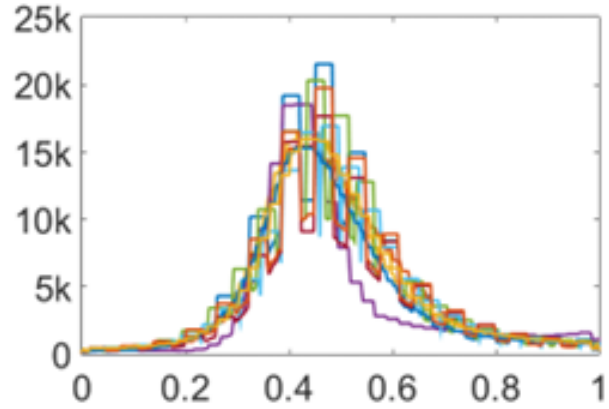

- Piece-wise linear: better alignment, but is it good for segmentation?

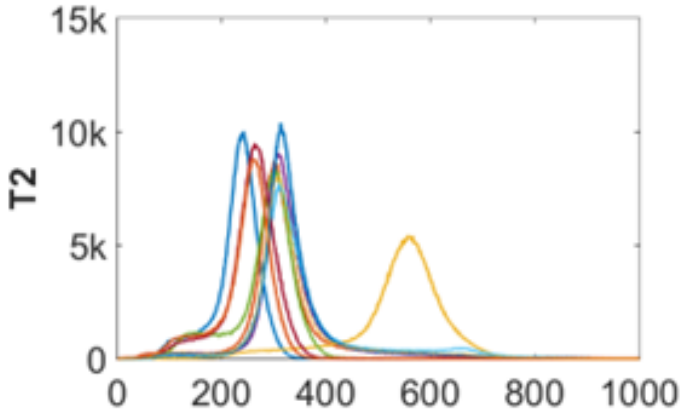

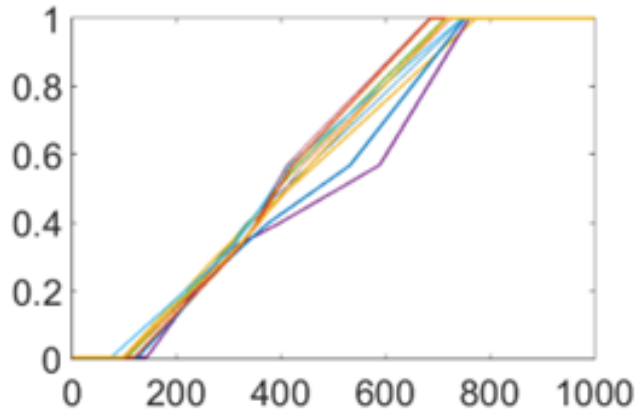

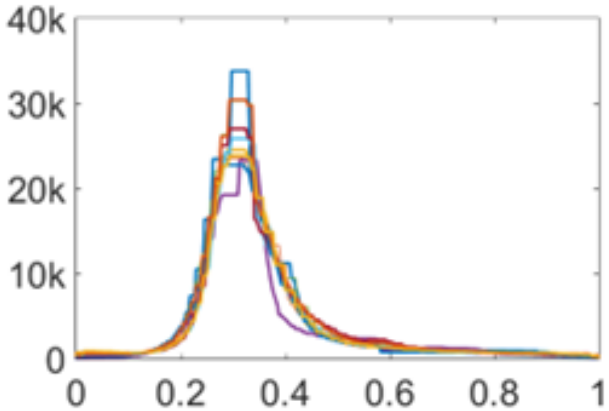

Parameters

- Linear transform (Alg. A1)
  - single parameter $\lambda_{25} \in [0.3, 0.5)$, $p_{25} \rightarrow \lambda_{25}$ and $p_{75} \rightarrow (1 - \lambda_{25})$
- Piece-wise linear transform (Alg. A2)
  - $p_{Lo} < 0.03, p_{Hi} = 1 - p_{Lo}$ what part to cut off at both ends
  - Set of landmark points
    - fixed points to be aligned

Scheme	Landmark points
M01	$p_{\mathrm{Lo}}, p_{50}, p_{\mathrm{Hi}}$
M02	$p_{\mathrm{Lo}}, p_{25}, p_{75}, p_{\mathrm{Hi}}$
M03	$p_{\mathrm{Lo}}, p_{25}, p_{50}, p_{75}, p_{\mathrm{Hi}}$
M04	$p_{\mathrm{Lo}}, p_{10}, p_{50}, p_{90}, p_{\mathrm{Hi}}$
M05	$p_{\mathrm{Lo}}, p_{20}, p_{40}, p_{60}, p_{80}, p_{\mathrm{Hi}}$
M06	$p_{\mathrm{Lo}}, p_{10}, p_{25}, p_{75}, p_{90}, p_{\mathrm{Hi}}$
M07	$p_{\mathrm{Lo}}, p_{20}, p_{35}, p_{50}, p_{65}, p_{80}, p_{\mathrm{Hi}}$
M08	$p_{\mathrm{Lo}}, p_{10}, p_{25}, p_{50}, p_{75}, p_{90}, p_{\mathrm{Hi}}$
M09	$p_{\mathrm{Lo}}, p_{10}, p_{25}, p_{40}, p_{60}, p_{75}, p_{90}, p_{\mathrm{Hi}}$
M10	$p_{\mathrm{Lo}}, p_{10}, p_{25}, p_{40}, p_{50}, p_{60}, p_{75}, p_{90}, p_{\mathrm{Hi}}$
M11	$p_{\mathrm{Lo}}, p_{10}, p_{20}, p_{30}, p_{40}, p_{60}, p_{70}, p_{80}, p_{90}, p_{\mathrm{Hi}}$
M12	$p_{\mathrm{Lo}}, p_{10}, p_{20}, p_{30}, p_{40}, p_{50}, p_{60}, p_{70}, p_{80}, p_{90}, p_{\mathrm{Hi}}$

Segmentation accuracy achieved with random forest classifier on iSeg-2017 data

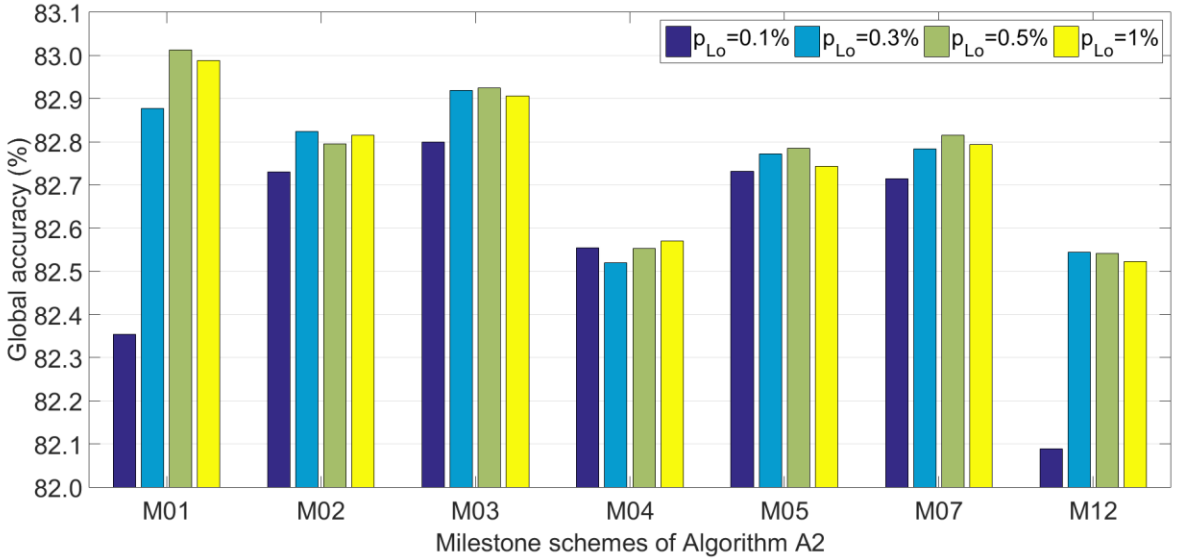

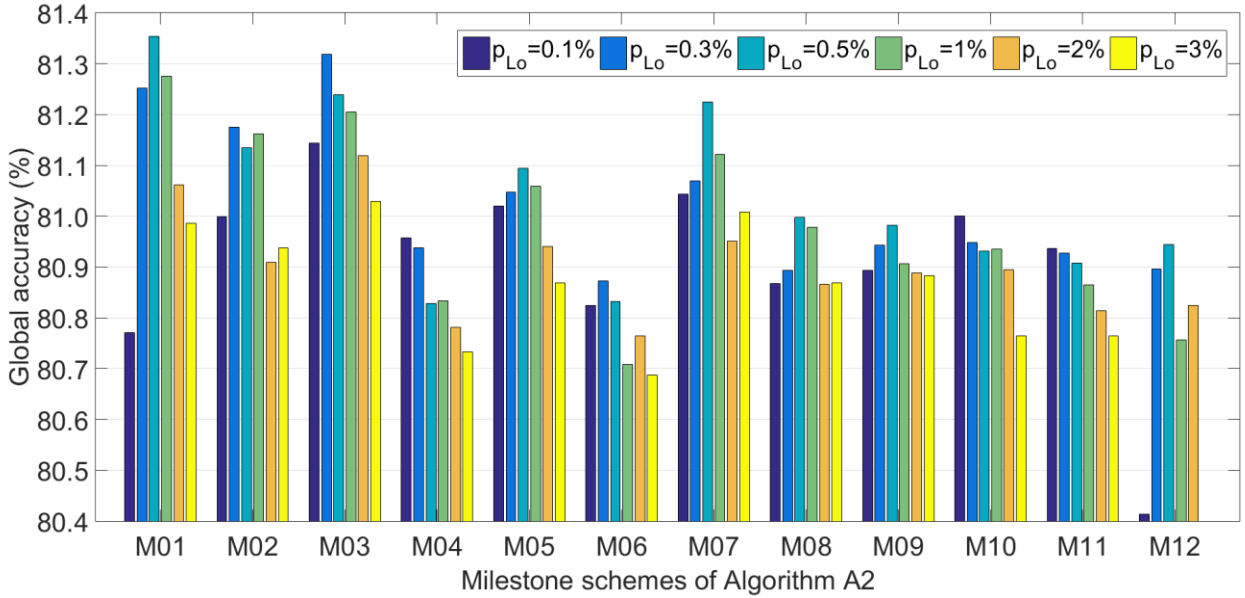

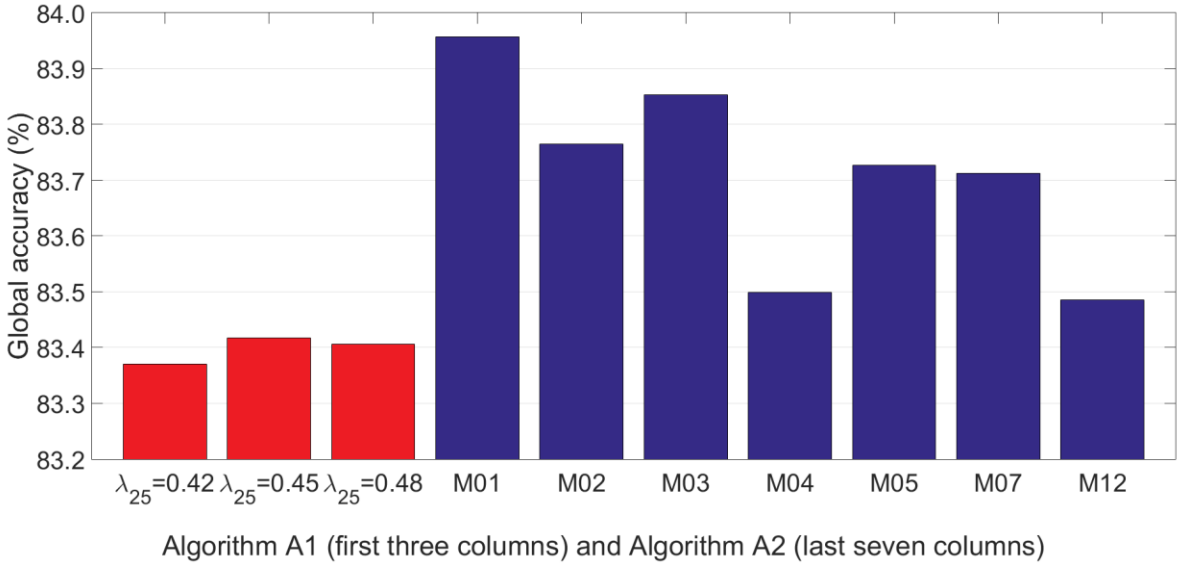

Before and after histogram alignment

Before After Before After

T1 T2 T1 T2 T1 T2 T1 T2

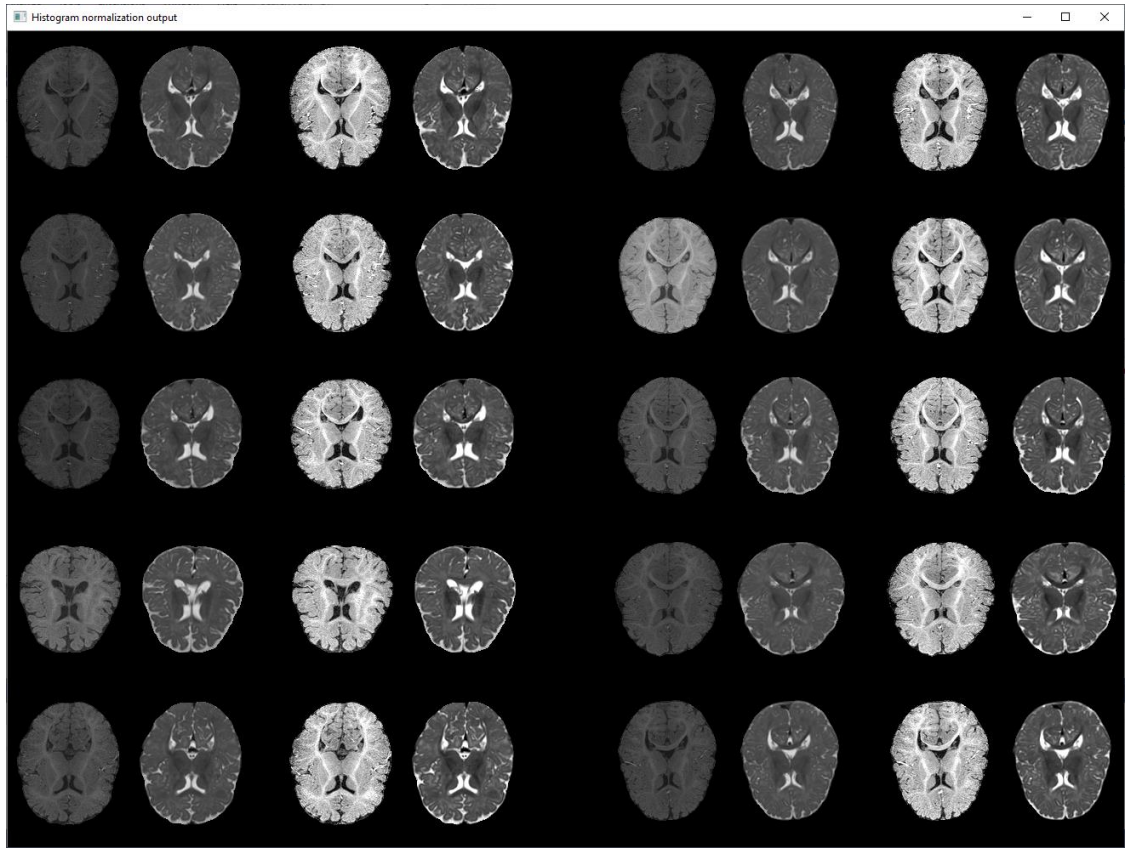

Before After

T1 T2 T1c FLAIR T1 T2 T1c FLAIR

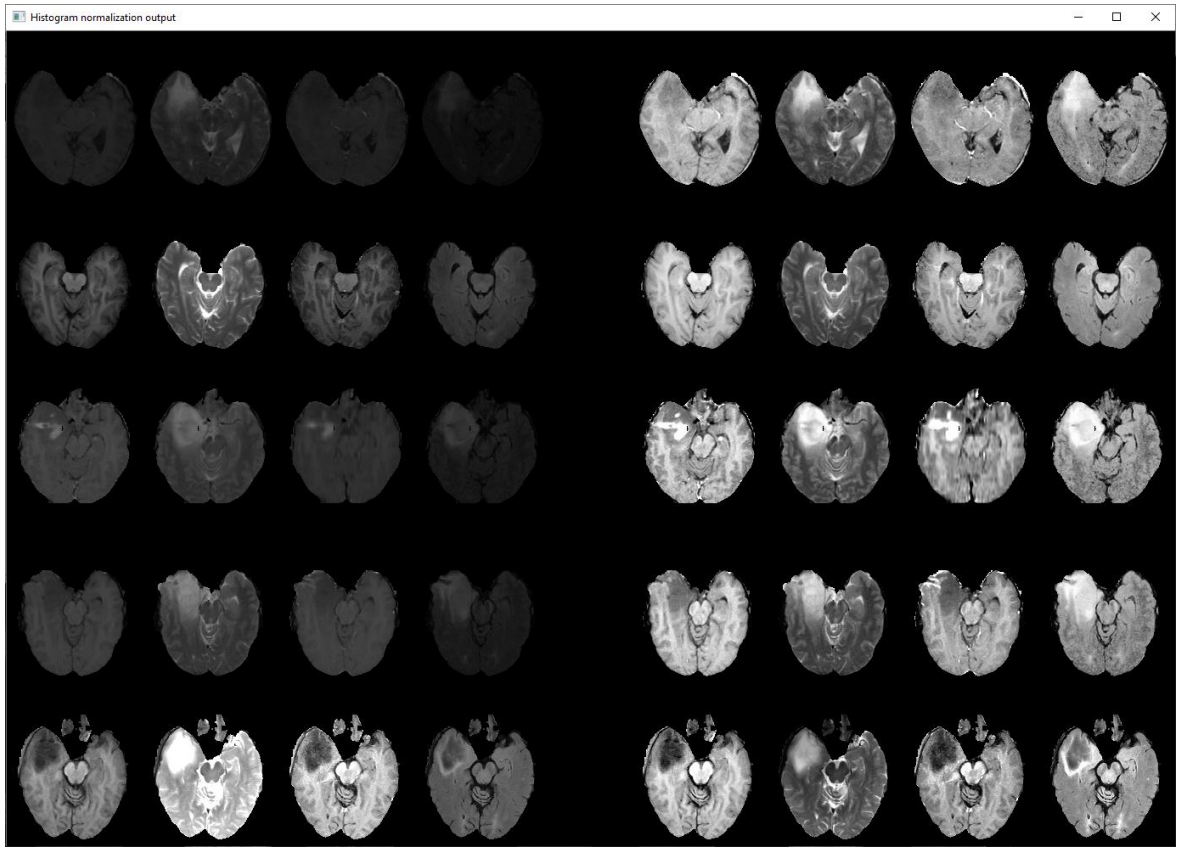

Recommendations

- Piece-wise linear transform (Nyúl et al) can perform better, but only if appropriately used
- Important issues
  - Not too many landmark points
  - Best schemes: M01, M03
  - No landmark points close to any ending od the histogram
  - better p_{20} than p_{10}, better p_{80} than p_{90}
- Most participants at early BraTS competitions did not set it properly
- Better accuracy, higher Dice score, up to 2% difference

Scheme	Landmark points
M01	$p_{\mathrm{Lo}}, p_{50}, p_{\mathrm{Hi}}$
M02	$p_{\mathrm{Lo}}, p_{25}, p_{75}, p_{\mathrm{Hi}}$
M03	$p_{\mathrm{Lo}}, p_{25}, p_{50}, p_{75}, p_{\mathrm{Hi}}$
M04	$p_{\mathrm{Lo}}, p_{10}, p_{50}, p_{90}, p_{\mathrm{Hi}}$
M05	$p_{\mathrm{Lo}}, p_{20}, p_{40}, p_{60}, p_{80}, p_{\mathrm{Hi}}$
M06	$p_{\mathrm{Lo}}, p_{10}, p_{25}, p_{75}, p_{90}, p_{\mathrm{Hi}}$
M07	$p_{\mathrm{Lo}}, p_{20}, p_{35}, p_{50}, p_{65}, p_{80}, p_{\mathrm{Hi}}$
M08	$p_{\mathrm{Lo}}, p_{10}, p_{25}, p_{50}, p_{75}, p_{90}, p_{\mathrm{Hi}}$
M09	$p_{\mathrm{Lo}}, p_{10}, p_{25}, p_{40}, p_{60}, p_{75}, p_{90}, p_{\mathrm{Hi}}$
M10	$p_{\mathrm{Lo}}, p_{10}, p_{25}, p_{40}, p_{50}, p_{60}, p_{75}, p_{90}, p_{\mathrm{Hi}}$
M11	$p_{\mathrm{Lo}}, p_{10}, p_{20}, p_{30}, p_{40}, p_{60}, p_{70}, p_{80}, p_{90}, p_{\mathrm{Hi}}$
M12	$p_{\mathrm{Lo}}, p_{10}, p_{20}, p_{30}, p_{40}, p_{50}, p_{60}, p_{70}, p_{80}, p_{90}, p_{\mathrm{Hi}}$

- CNN based methods only need enhancement of visibility
- Contrast Limited Adaptive Histogram Equalization (CLAHE)

Spectral resolution

- What is the effect of color depth upon segmentation quality?
- How many bits are useful?
- Observed MRI data come at 16-bit resolution

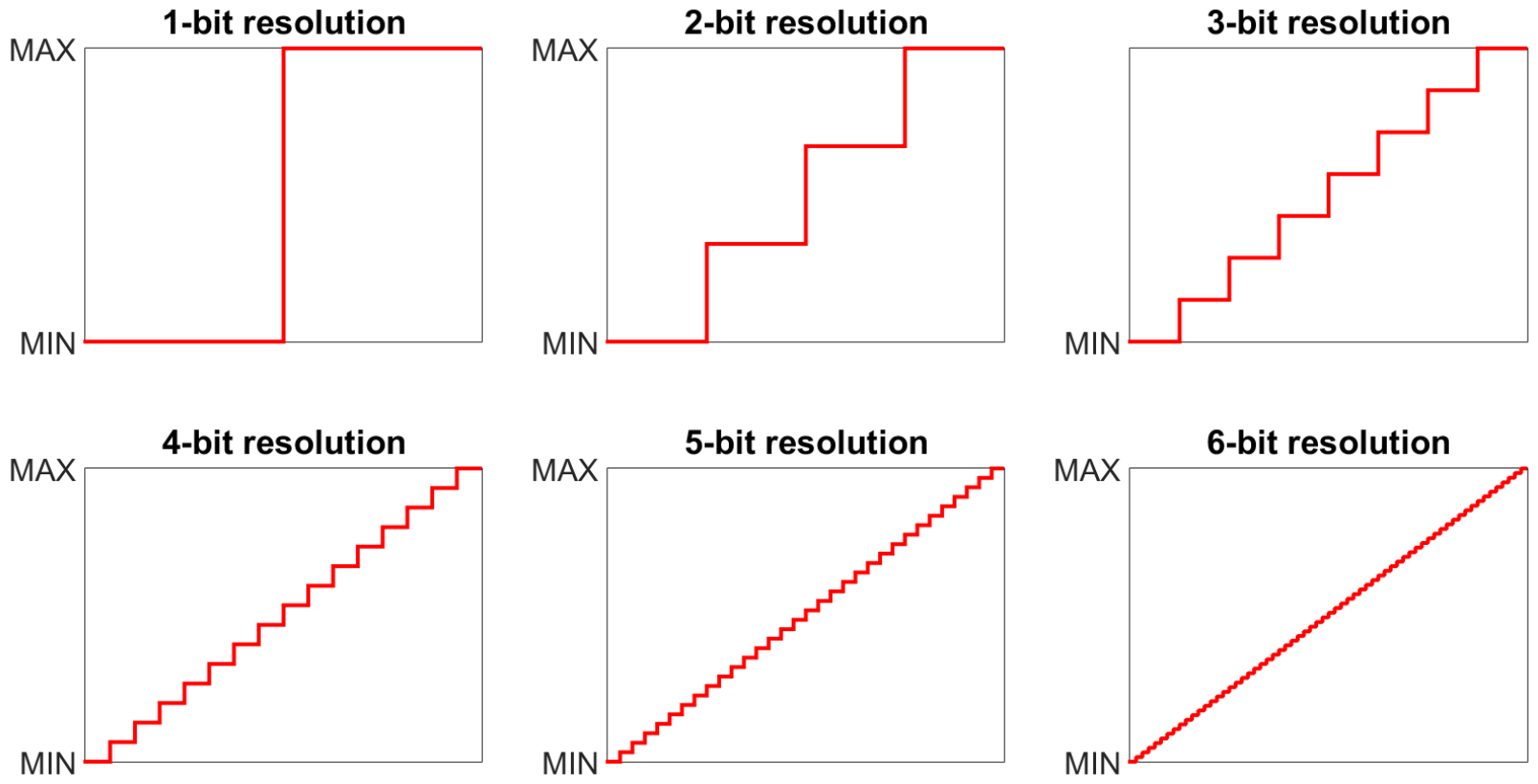

MRI data represented at 2 to 8 bits spectral resolution

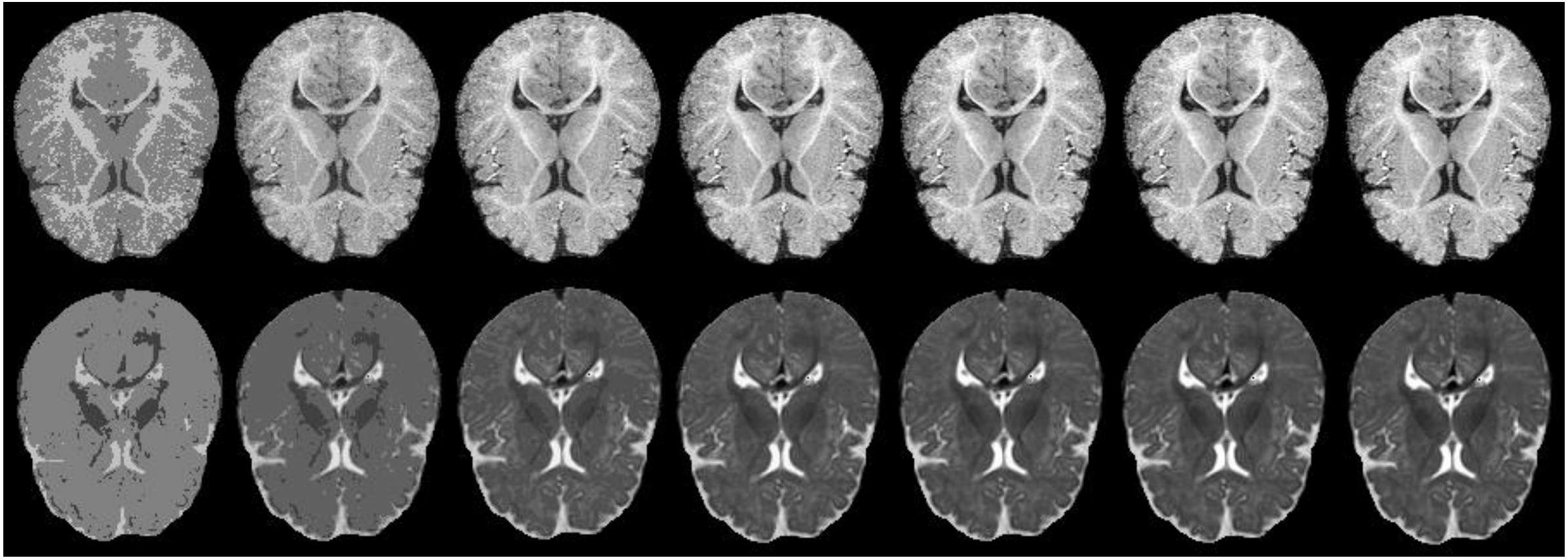

2 bits 3 bits 4 bits 5 bits 6 bits 7 bits 8 bits

Results

- Above 6-bit resolution the segmentation quality saturates
- Multi-channel preprocessed data can be efficiently stored in single byte per feature
- Reduce the archive storage space by 50%

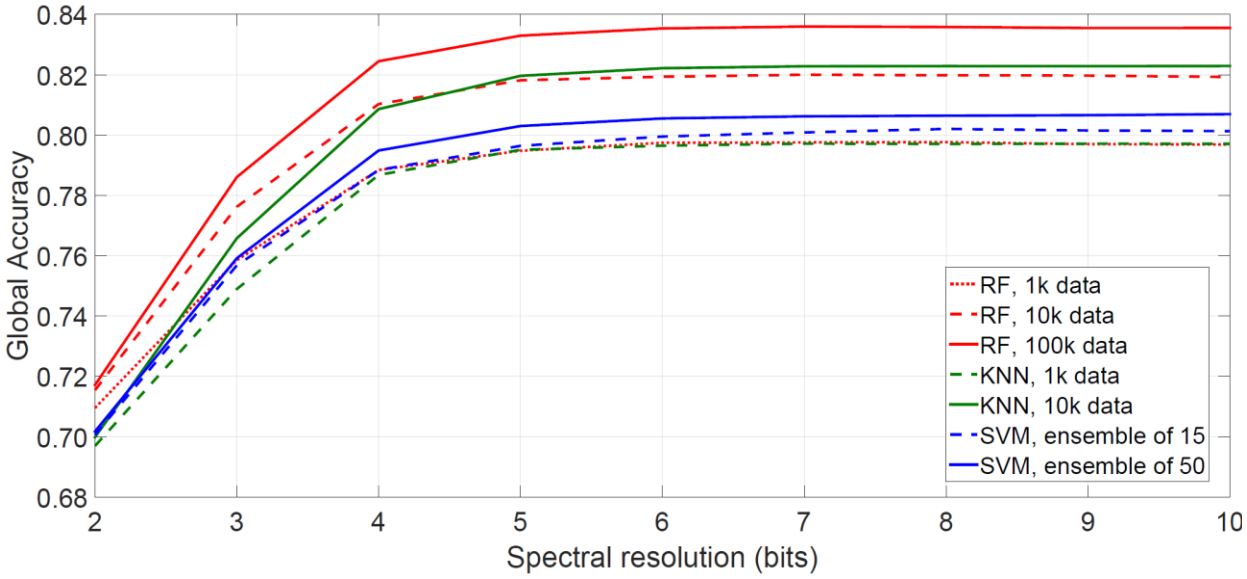

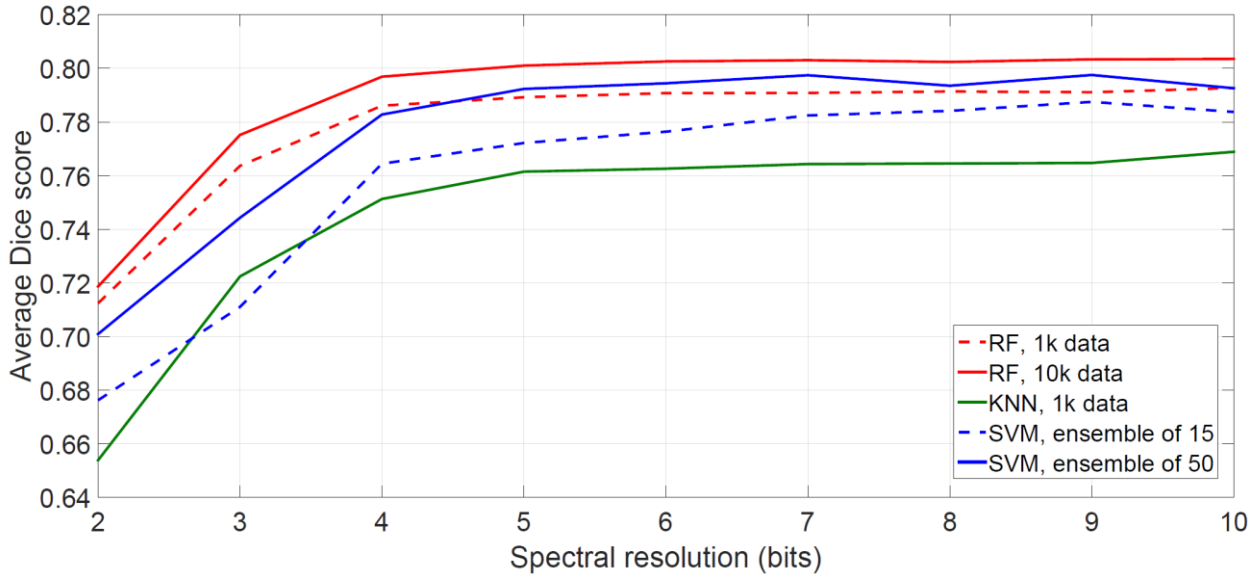

Feature generation and selection

- CNN-based methods extract the features they use
- Classical machine learning based methods use handcrafted features
- 4 observed features (T1, T2, T1C, FLAIR)
- 4 x 25 = 100 computed features

Neighborhood	Average	Maximum	Minimum	Median	Gradient	Gabor	Total
$3 \times 3 \times 3$	4	4	4				12
3×3	4			4			8
5×5	4			4			8
7×7	4			4	16		24
9×9	4			4			8
11×11	4			4		32	40
Total	24	4	4	20	16	32	100

Feature selection

- Markov clustering based on pairwise “similarity” data
- Similarity of features
  - How often they appear together in making a decision
  - How often these decisions are correct

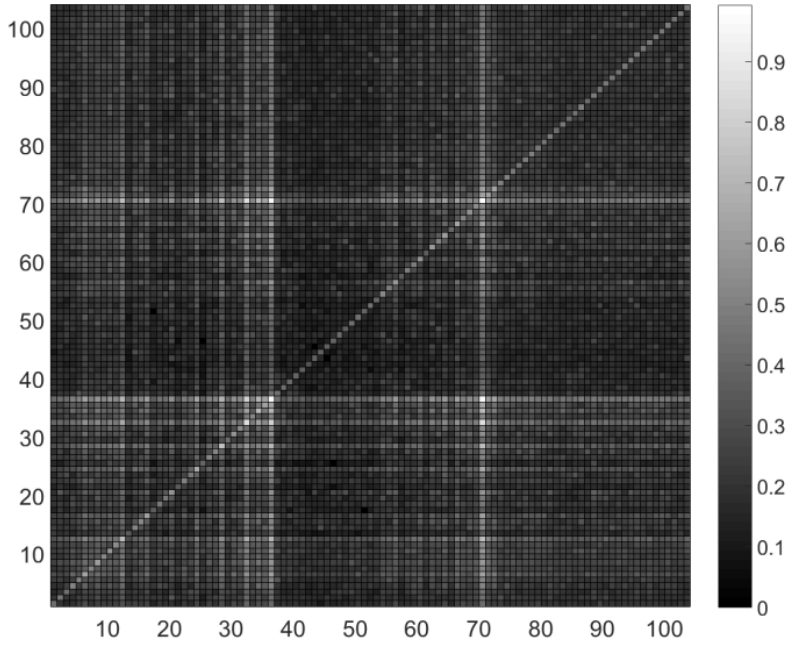

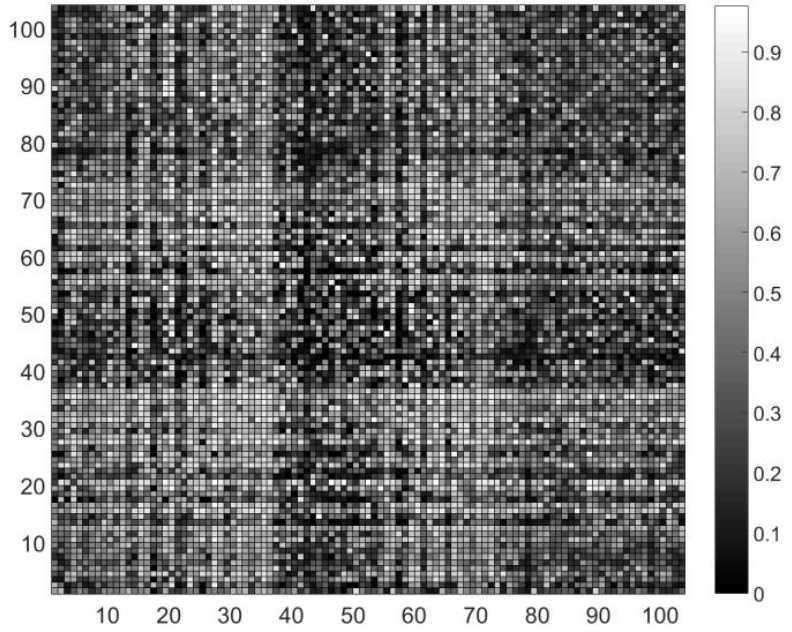

Reduced sets of features

- Markov clustering has a single parameter: inflation rate r
- Size of largest cluster of features depends on r

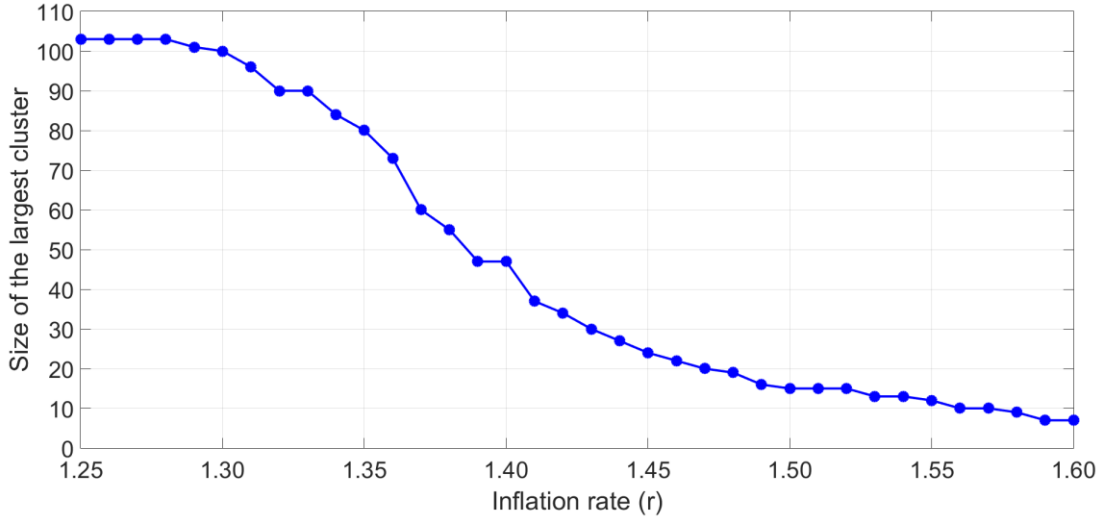

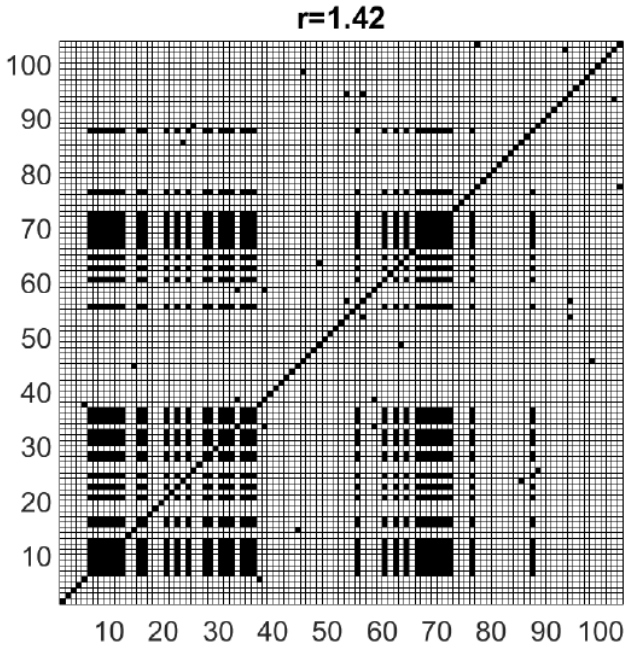

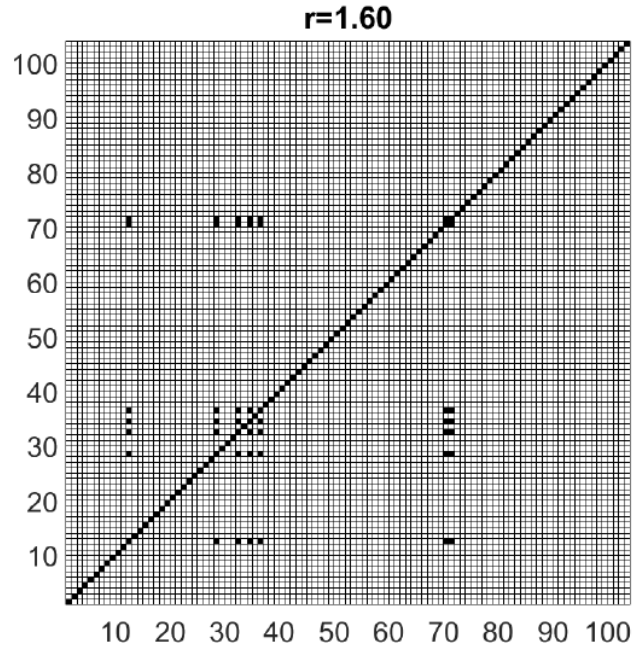

Segmentation quality

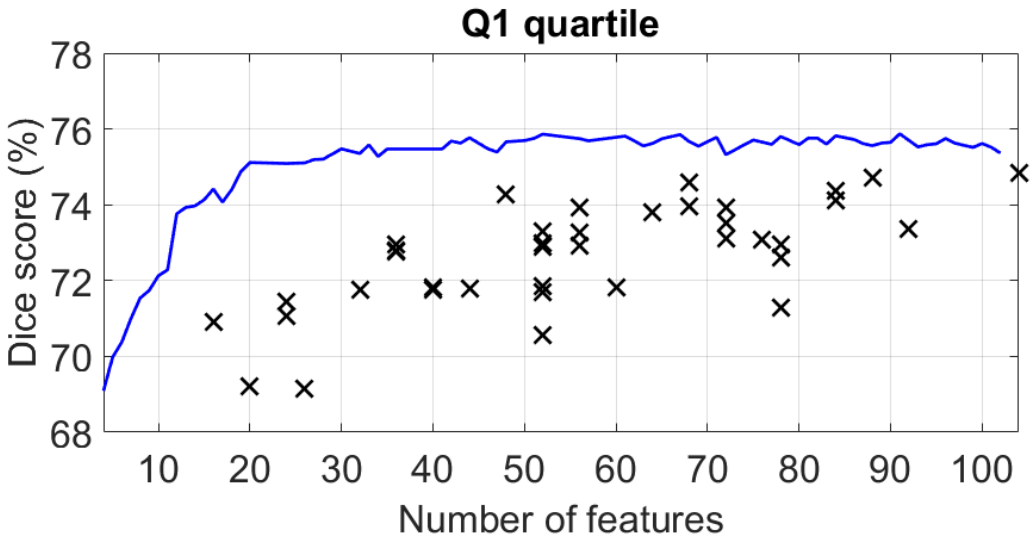

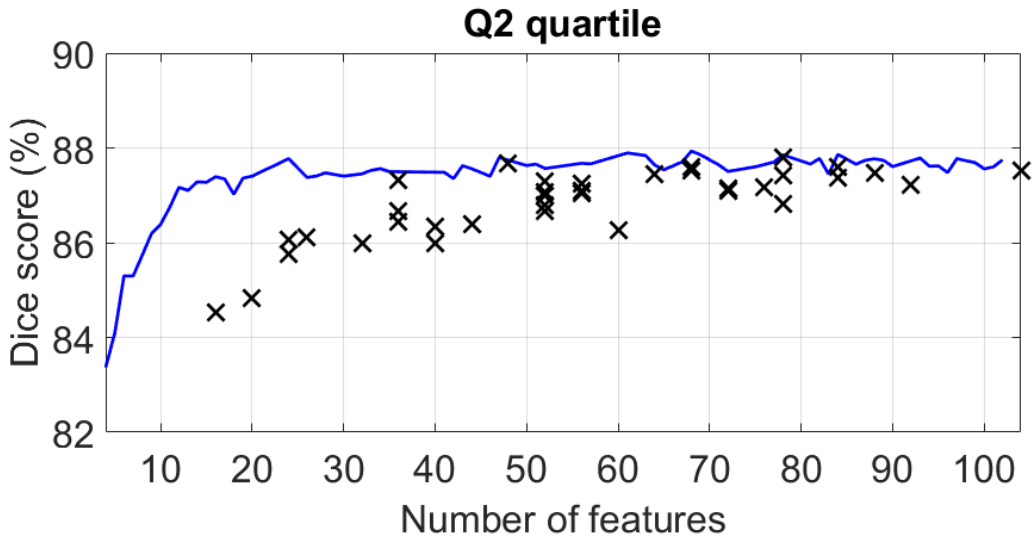

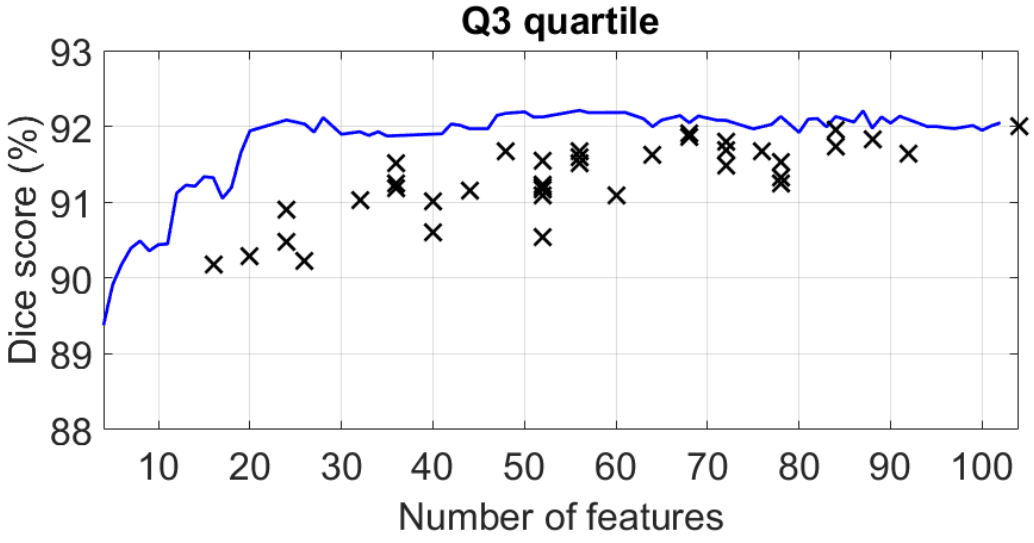

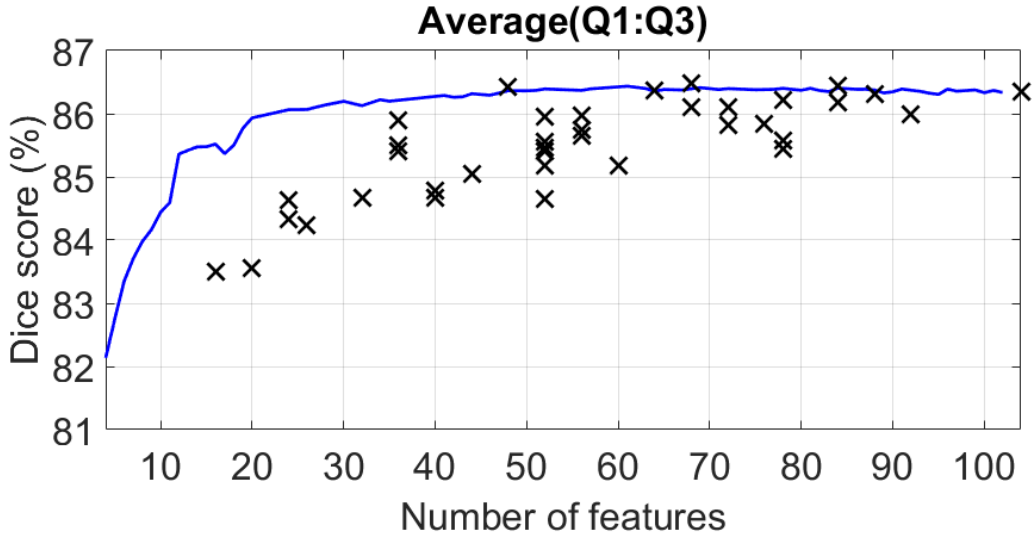

	11 features	26 features	41 features	104 features
False Positives	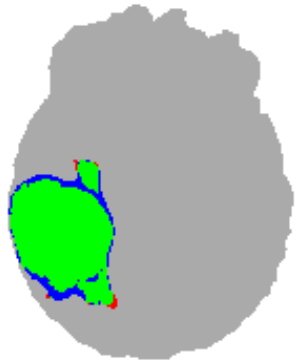	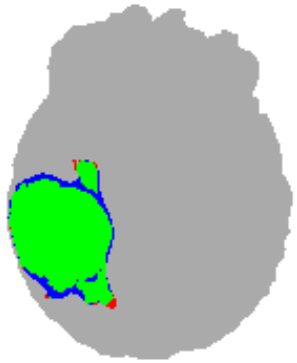	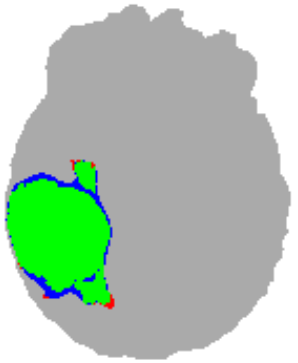	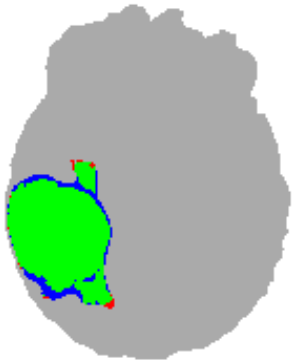
True Positives	336 2206 28	309 2200 34	292 2197 37	295 2198 36
	DSC=92.38%	DSC=92.77%	DSC=93.03%	DSC=92.99%
False Negatives	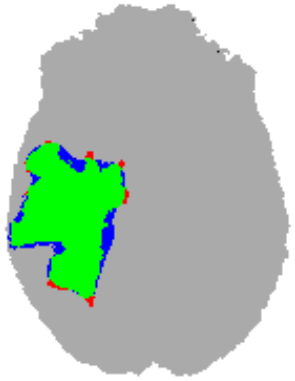	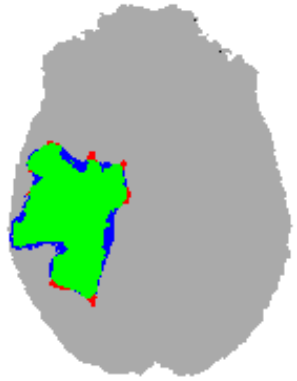	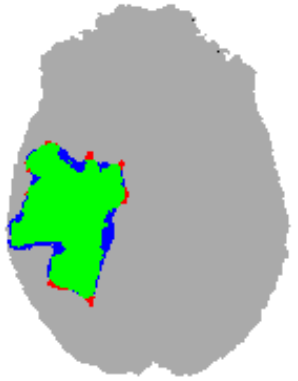	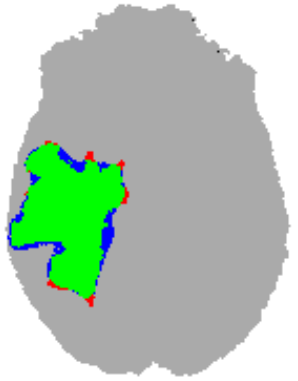
Dice Score	348 2240 70	321 2229 81	337 2231 79	322 2228 82
	DSC=91.47%	DSC=91.73%	DSC=91.47%	DSC=91.69%

Segmentation results (TP FP FN)

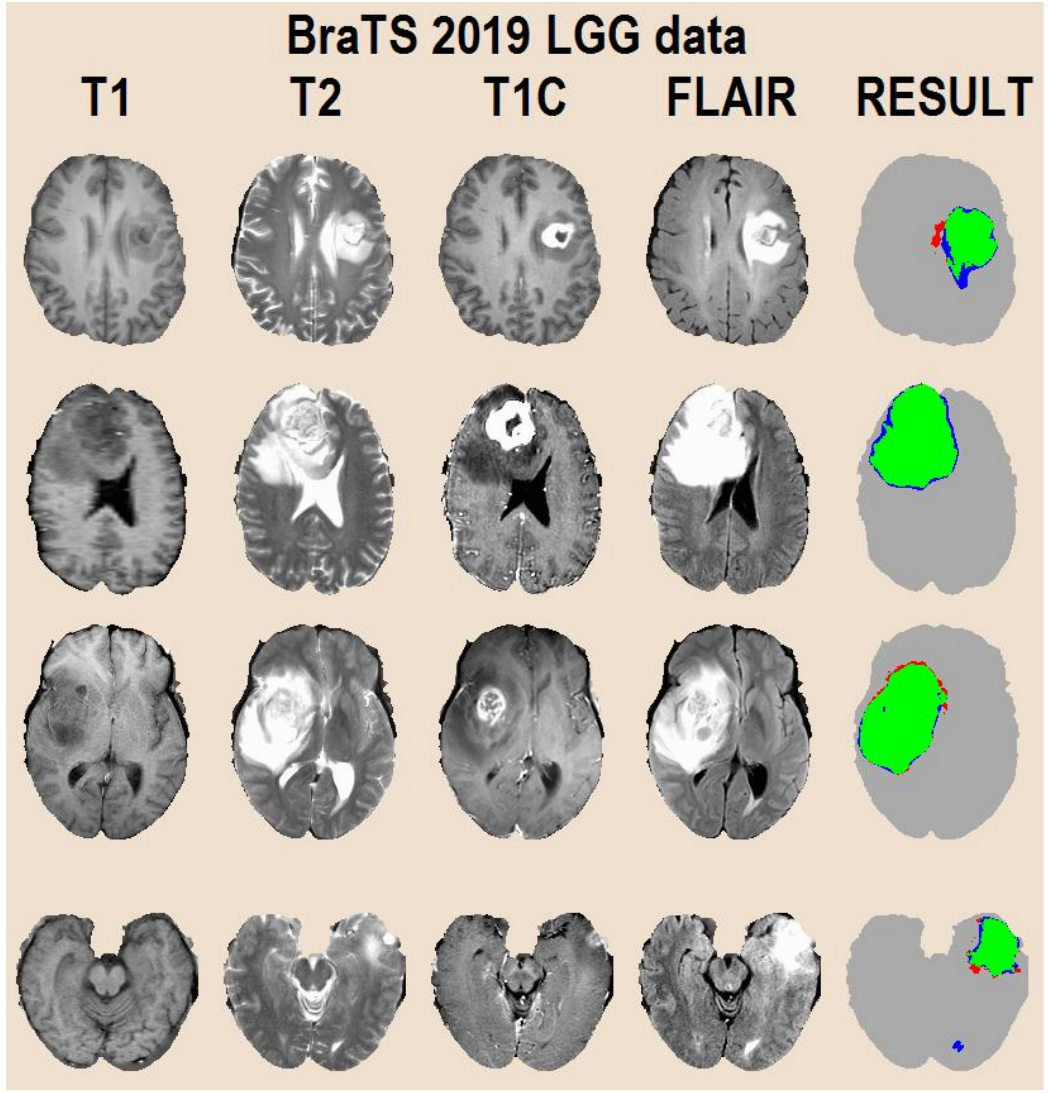

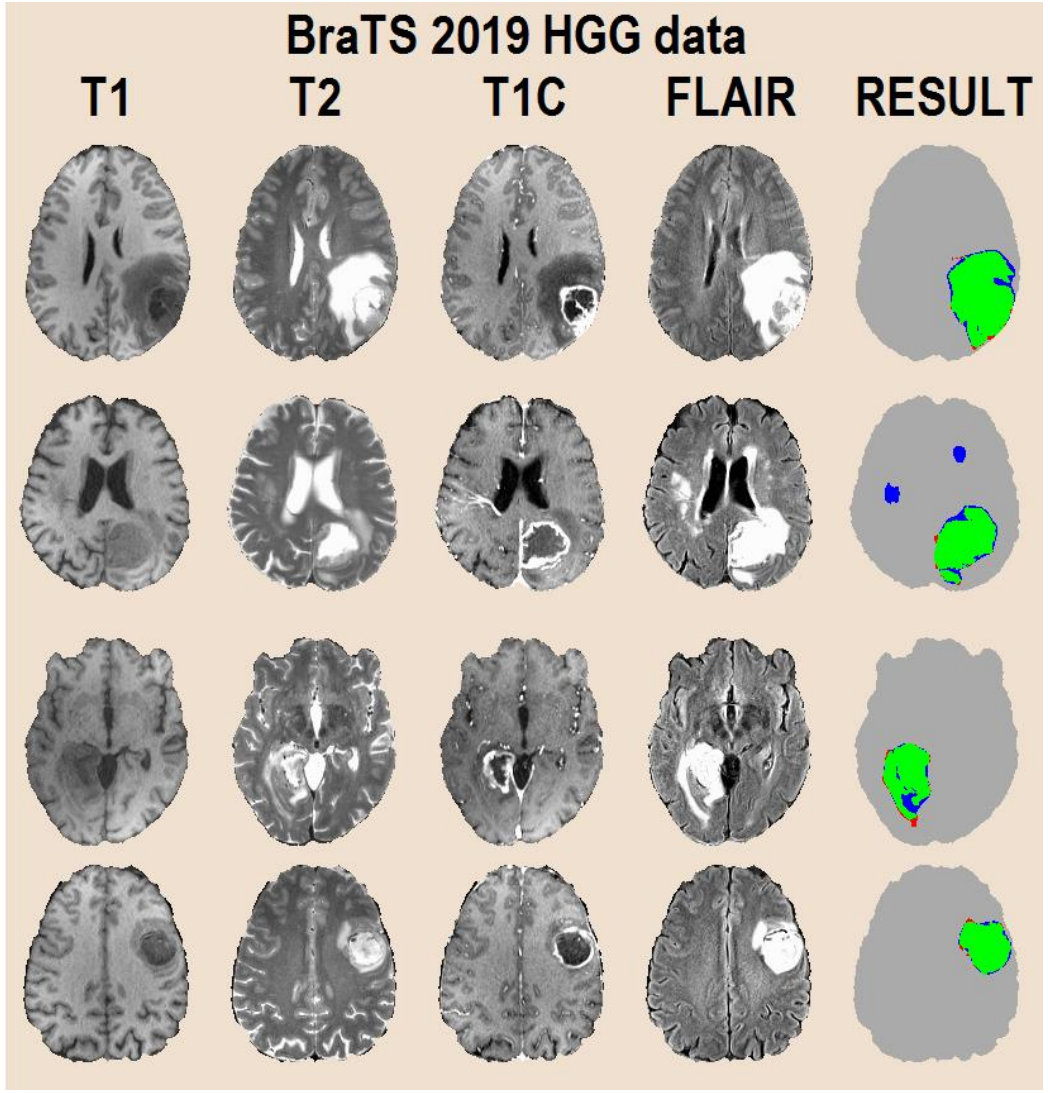

Segmentation accuracy vs. tumor size (HGG)

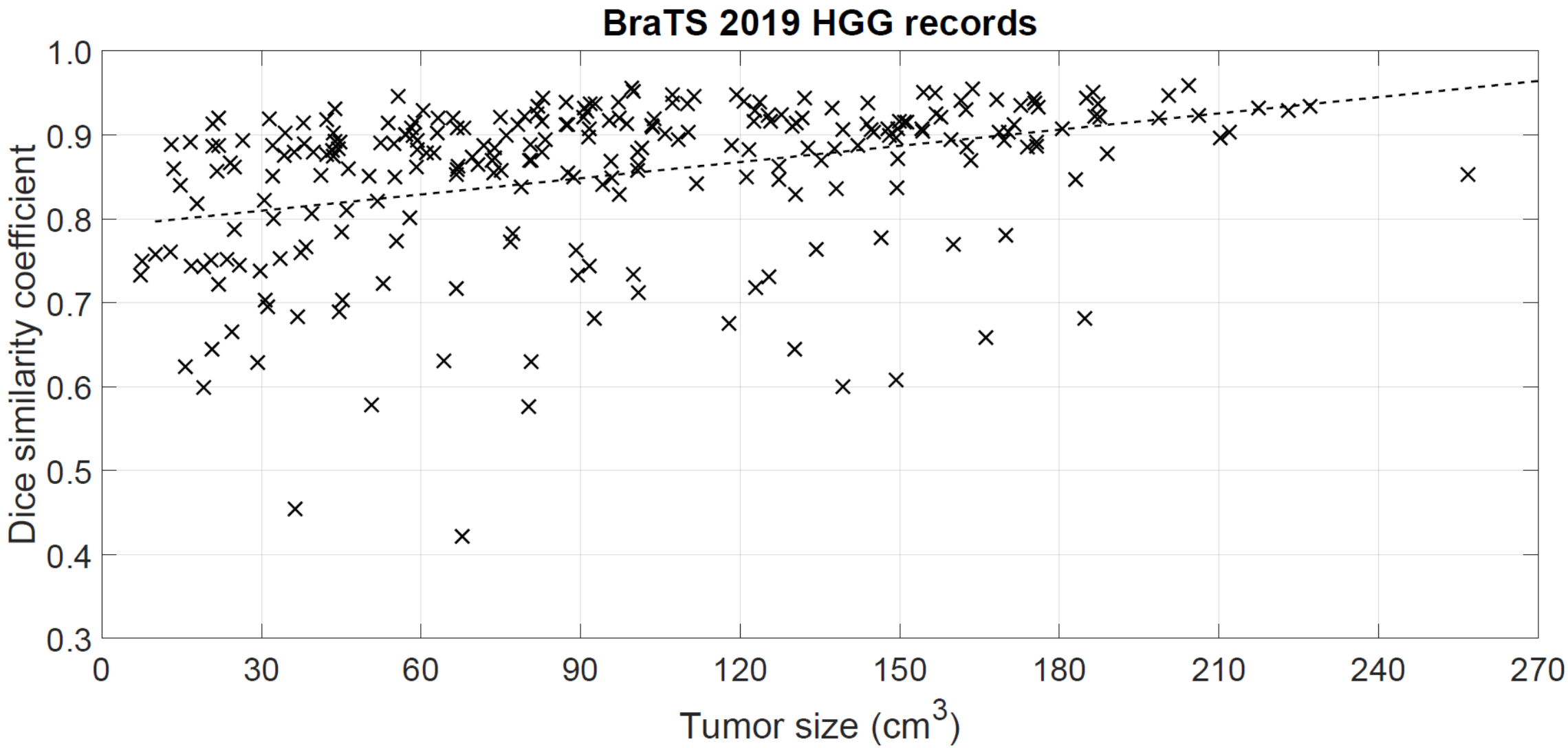

U-net architecture

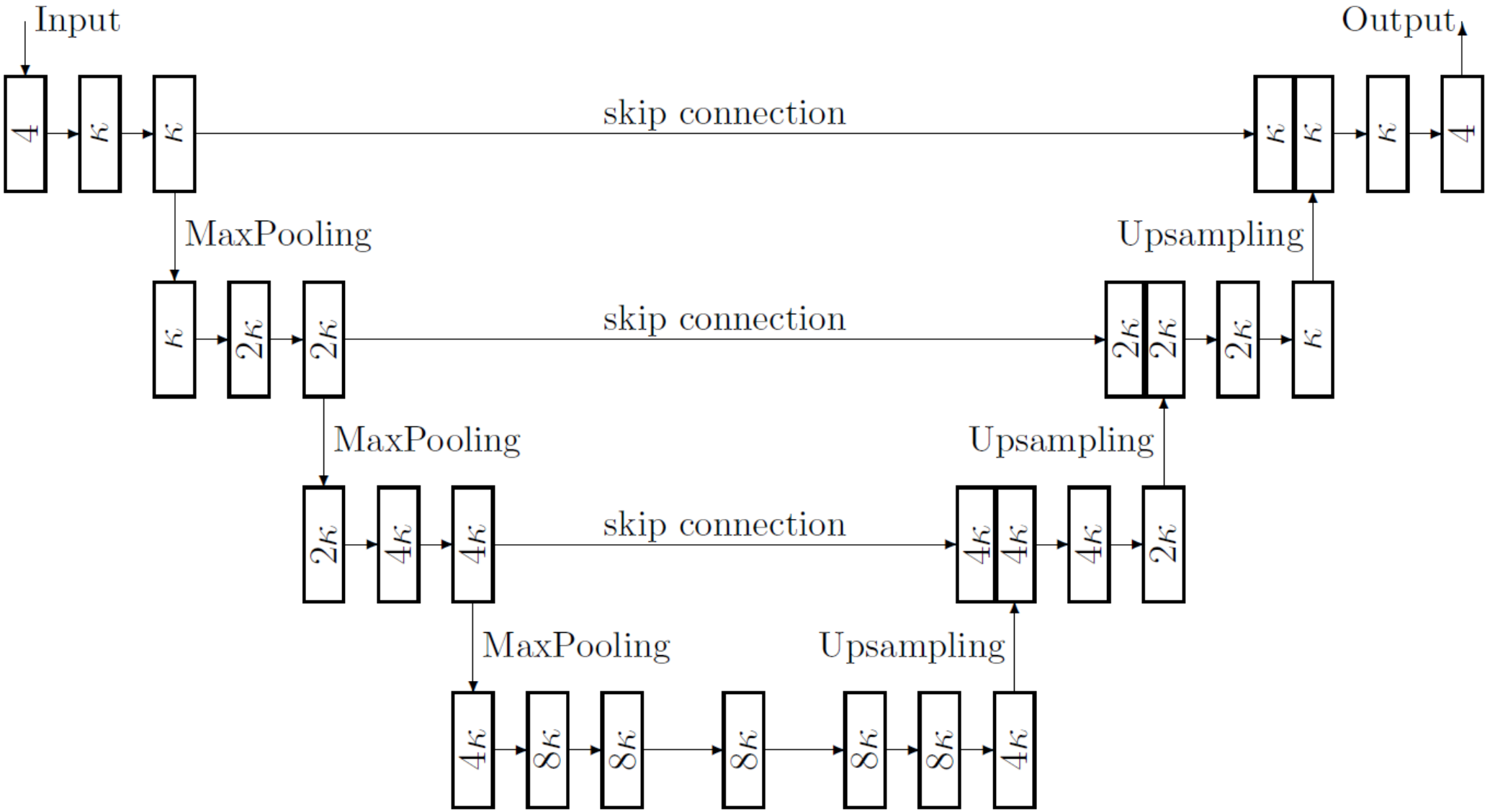

Proposed cascade

- First U-net performs a segmentation of preprocessed MRI data
- Second U-net performs post-processing using features extracted from the first segmentation outcome
- Feature extraction: percentage of positive pixels within 3x3x3, 5x5x5, 7x7x7, 9x9x9 sized neighborhoods

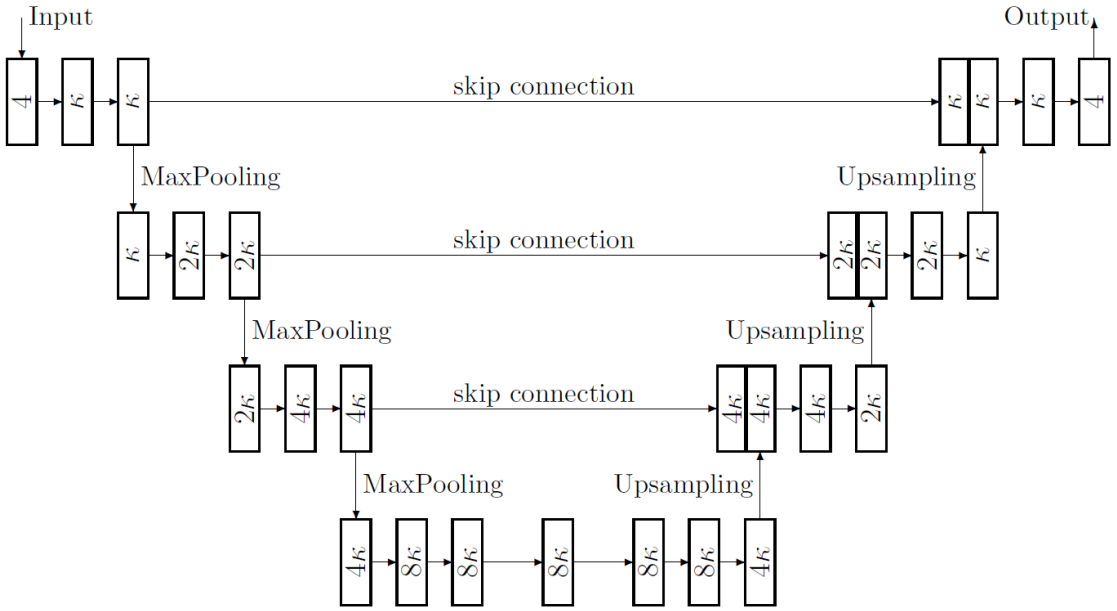

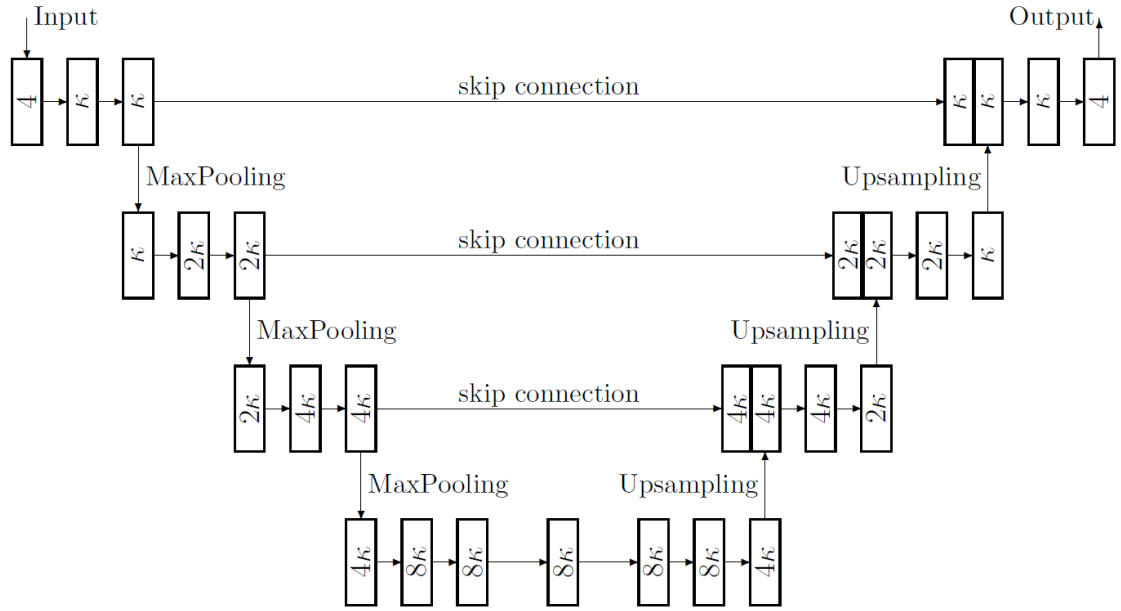

Data flow

- Dataset divided in two equal groups
- Data A, B
- Label L_A, L_B
- Initial segmentations S_A, S_B
- Features F_A, F_B
- Final segmentations S'_A, S'_B
- A and B can swap roles

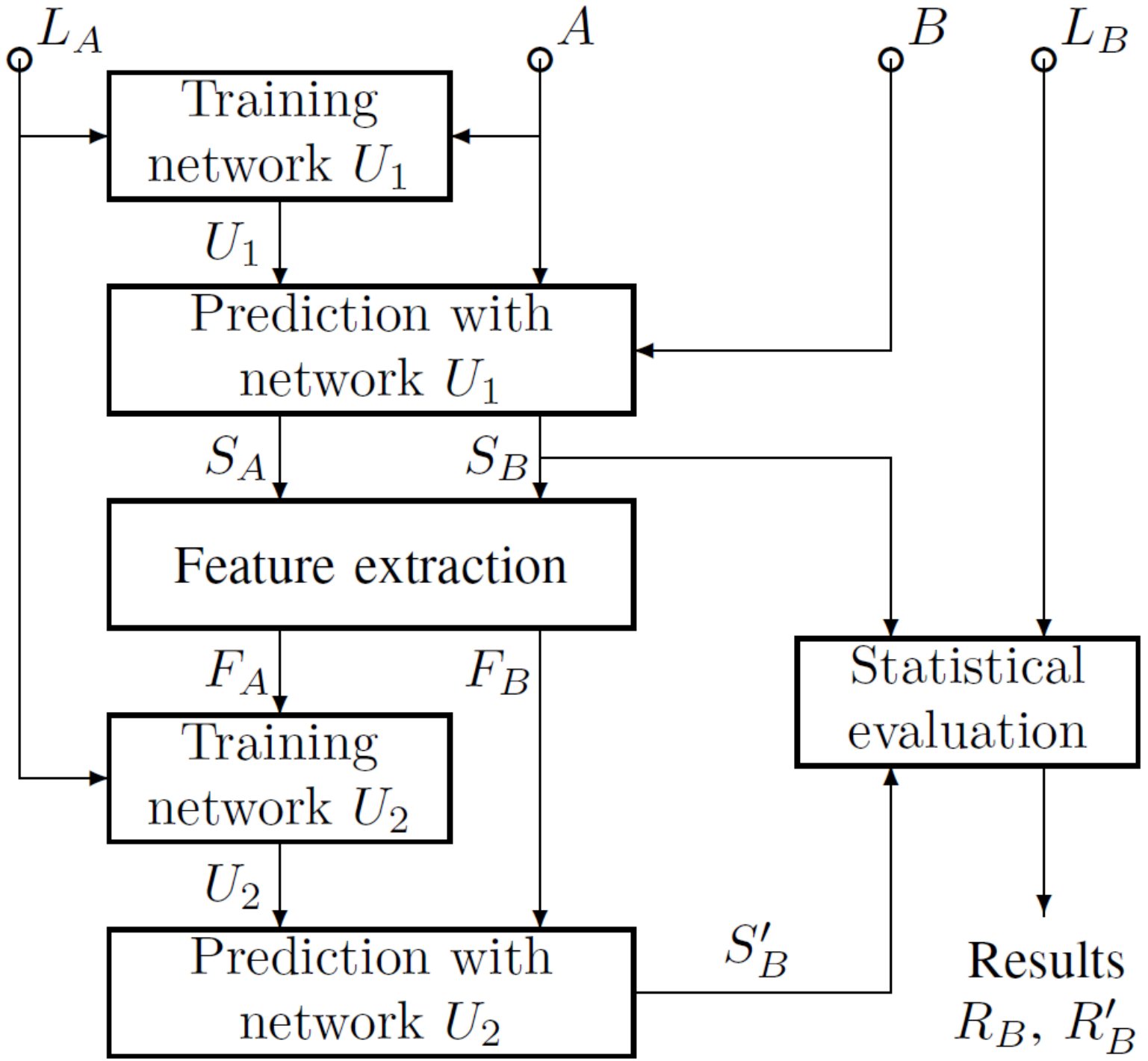

Measuring accuracy

- Based on ground truth and final decision: TP, TN, FP, FN
- Accuracy indicators: DSC, TPR, TNR, ACC

Indicator	Formula
True positive rate	$\mathrm{TPR}_i = \frac{\mathrm{TP}_i}{\mathrm{TP}_i+\mathrm{FN}_i}$
True negative rate	$\mathrm{TNR}_i = \frac{\mathrm{TN}_i}{\mathrm{TN}_i+\mathrm{FP}_i}$
Positive predictive value	$\mathrm{PPV}_i = \frac{\mathrm{TP}_i}{\mathrm{TP}_i+\mathrm{FP}_i}$
Dice score or F_1-score	$\mathrm{DSC}_i = \frac{2\times\mathrm{TP}_i}{2\times\mathrm{TP}_i+\mathrm{FP}_i+\mathrm{FN}_i}$
Accuracy	$\mathrm{ACC}_i = \frac{\mathrm{TP}_i+\mathrm{TN}_i}{\mathrm{TP}_i+\mathrm{TN}_i+\mathrm{FP}_i+\mathrm{FN}_i}$

- Individual value for each volume (record)
- Average, SD, quartiles

Overall accuracy indicators

	Value	DSC	TPR	PPV	TNR	ACC
Before PP	average	0.8768	0.8662	0.9057	0.9920	0.9864
	stdev	0.0776	0.1154	0.0961	0.0073	0.0094
	1st quartile	0.8503	0.8214	0.8751	0.9888	0.9836
	median	0.9024	0.8868	0.9338	0.9935	0.9891
	3rd quartile	0.9302	0.9548	0.9757	0.9973	0.9921
After PP	average	0.8879	0.8665	0.9251	0.9913	0.9870
	stdev	0.0767	0.1108	0.0819	0.0085	0.0094
	1st quartile	0.8612	0.8303	0.9070	0.9891	0.9834
	median	0.9116	0.8957	0.9531	0.9939	0.9901
	3rd quartile	0.9380	0.9398	0.9749	0.9964	0.9932

Parameter selection

DSC	Layer depth parameter κ						
	16	32	48	64	80	96	112
average	0.8568	0.8702	0.8725	0.8629	0.8707	0.8768	0.8688
stdev	0.0868	0.0757	0.0769	0.0944	0.0780	0.0774	0.0798
1st quartile	0.8255	0.8509	0.8464	0.8386	0.8379	0.8503	0.8419
median	0.8809	0.8942	0.8956	0.8921	0.8942	0.9024	0.8910
3rd quartile	0.9164	0.9215	0.9260	0.9240	0.9263	0.9302	0.9259
ranked 1st	15	29	33	19	23	58	62
ranked 2nd	20	39	26	31	52	52	19
ranked 3rd	15	23	41	33	59	33	35
Total	50	91	100	83	134	143	116
$\mathrm{DSC}_i > 0.93$	31	40	52	47	52	61	51
$\mathrm{DSC}_i > 0.9$	86	109	110	105	112	122	107
$\mathrm{DSC}_i > 0.85$	160	181	177	170	175	180	169
$\mathrm{DSC}_i > 0.8$	193	201	203	196	204	202	200

Accuracy Indicators for Individual Volumes

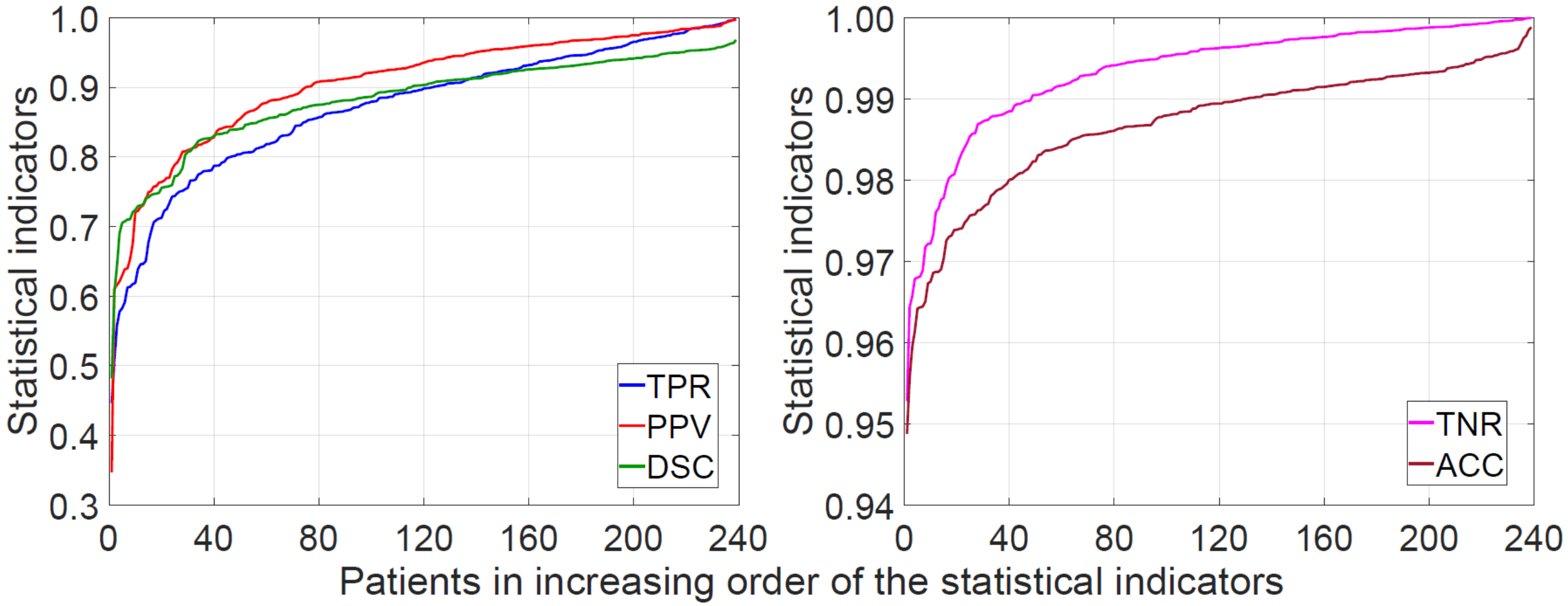

Effect of Post-processing

Tumor size	Before PP	After PP
10 cm^3	0.8147	0.8622
20 cm^3	0.8212	0.8643
50 cm^3	0.8405	0.8706
100 cm^3	0.8728	0.8811

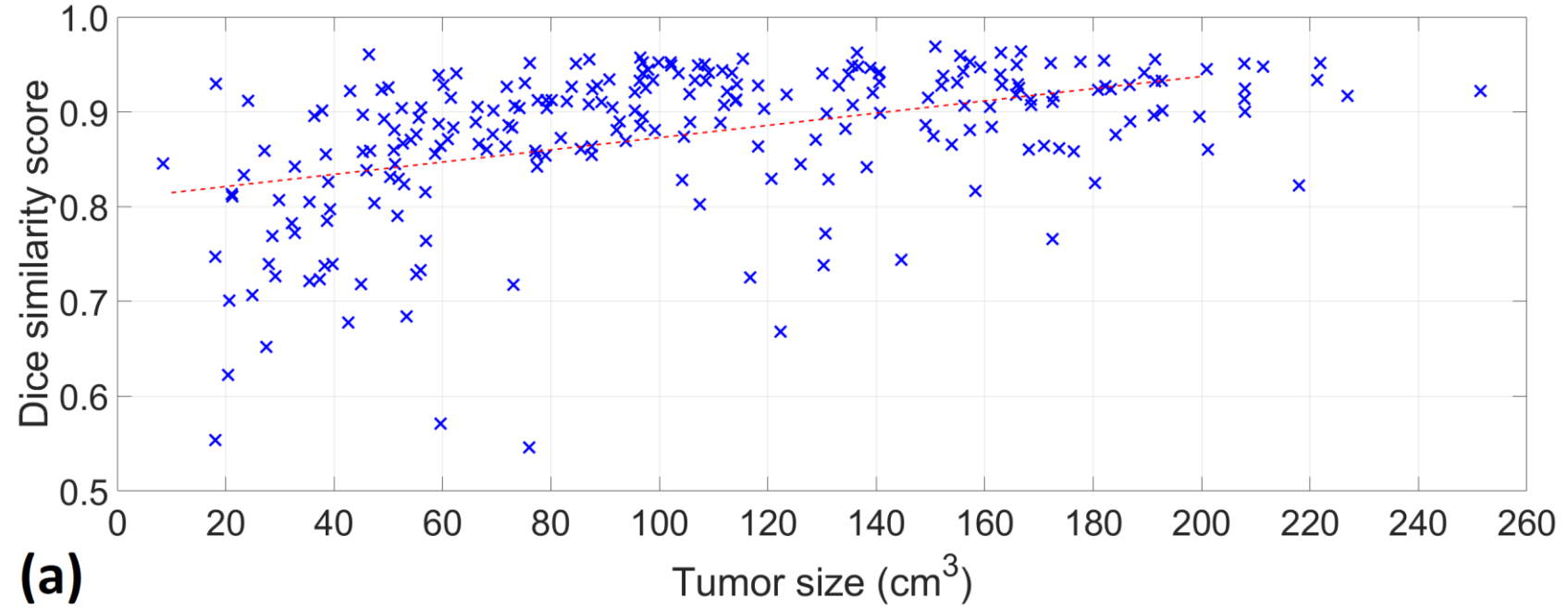

(a)

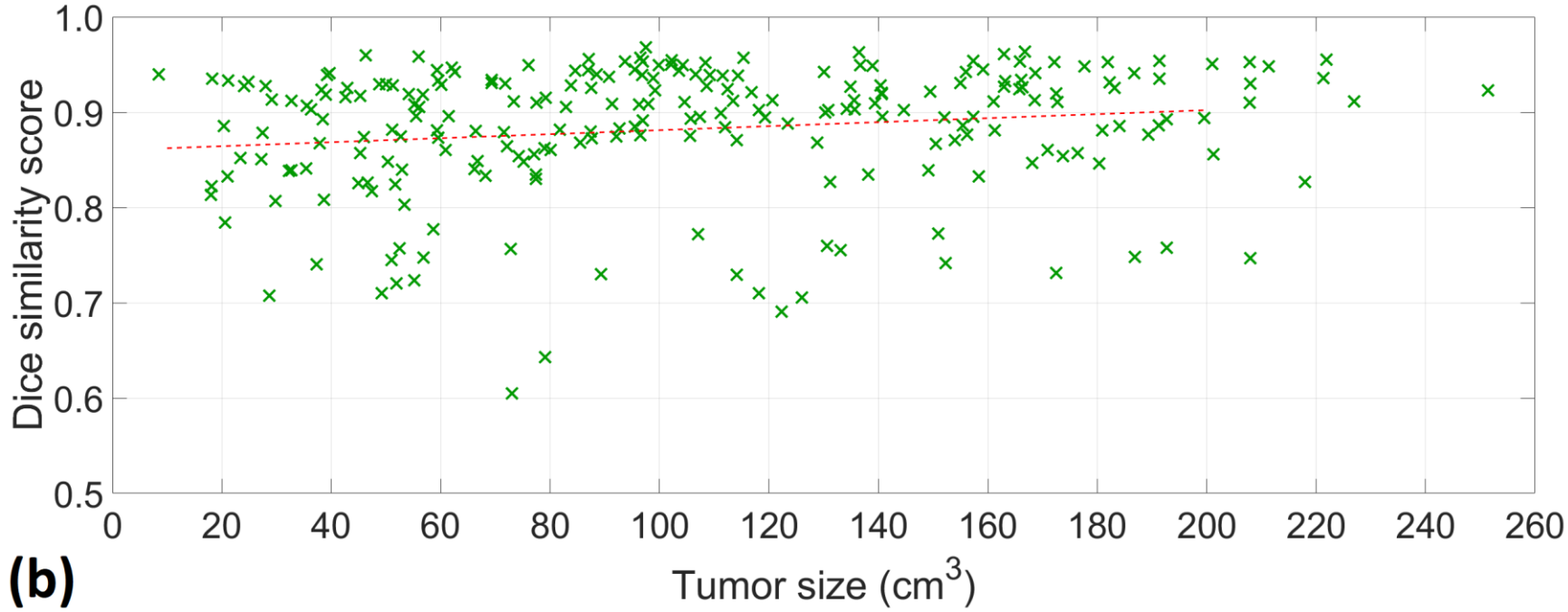

(b)

Detected tumors: TP FP FN

Input

Preprocessed

Segmented

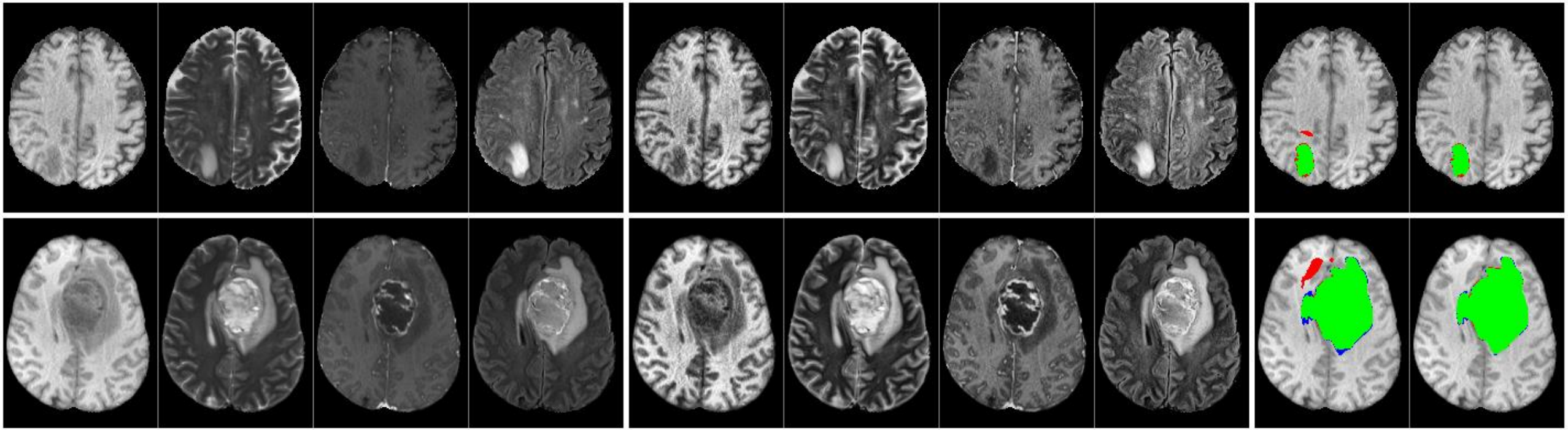

Comparison

Paper	Classifier	Data	Mean DSC
Tustison et al. [10] (2015)	RF, MRF	BraTS 2013	0.87
Pereira et al. [17] (2016)	CNN		0.88
Lefkovits et al. [30] (2017)	RF		0.868
Havaei et al. [31] (2017)	deep CNN		0.88
Pinto et al. [14] (2018)	ERT		0.85
Pereira et al. [32] (2019)	FCNN		0.86
Pereira et al. [17] (2016)	CNN	BraTS 2015	0.78
Kamnitsas et al. [20] (2017)	deep CNN		0.849
Zhao et al. [18] (2018)	FCNN, CRF		0.84
Chen et al. [33] (2019)	CNN		0.85
Ding et al. [34] (2019)	deep ResNet		0.86
Wu et al. [19] (2020)	CNN		0.83
Győrfi et al. [35] (2021)	BDT ensemble		0.8355
Bhalerao et al. [36] (2020)	3D Residual U-Net	BraTS 2019/20	0.85269
Wang et al. [37] (2020)	3D U-Net		0.894
Guo et al. [38] (2020)	CNN + fusion		0.872
Győrfi et al. [35] (2021)	BDT ensemble		0.8516
Lefkovits et al. [39] (2022)	CNN ensemble		0.8780
Proposed method	U-net cascade		0.8879

Dice similarity scores of various tumor parts

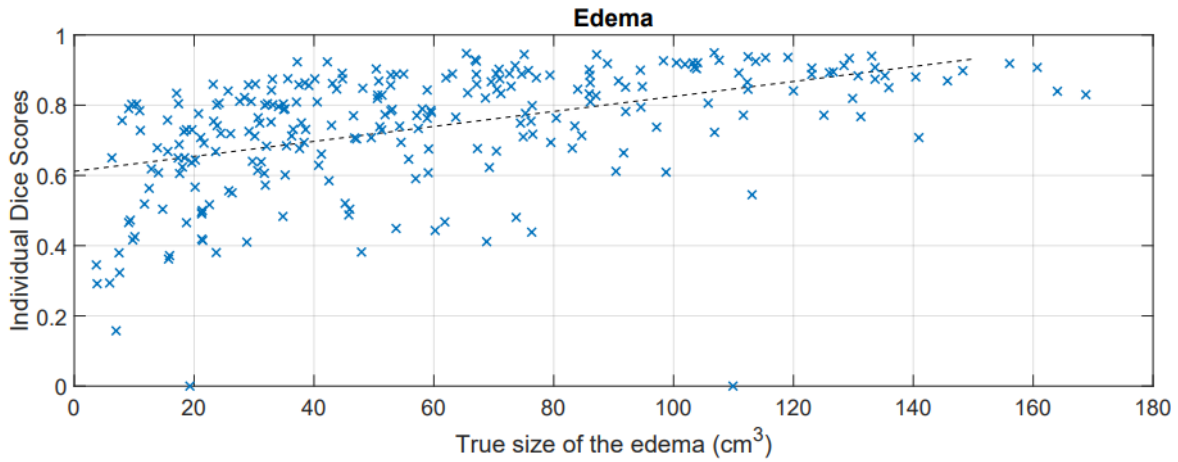

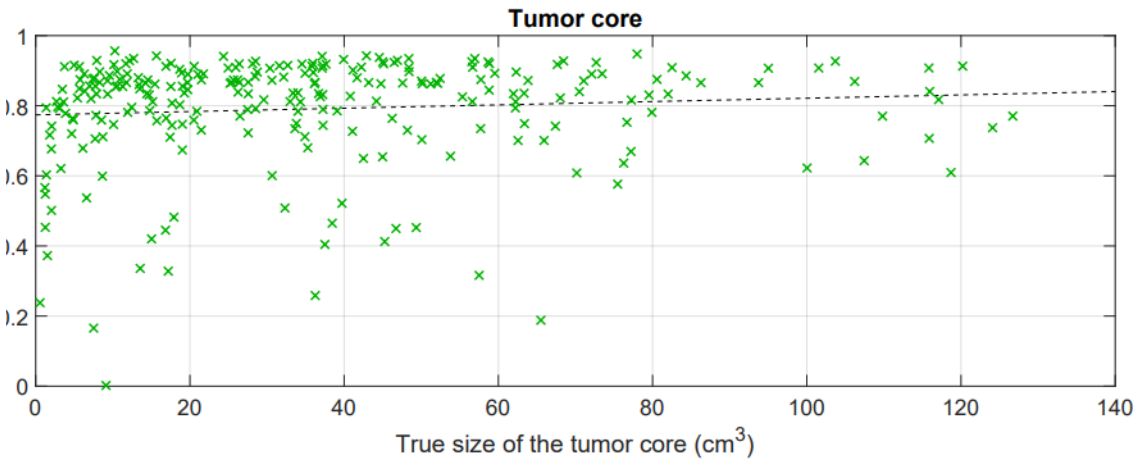

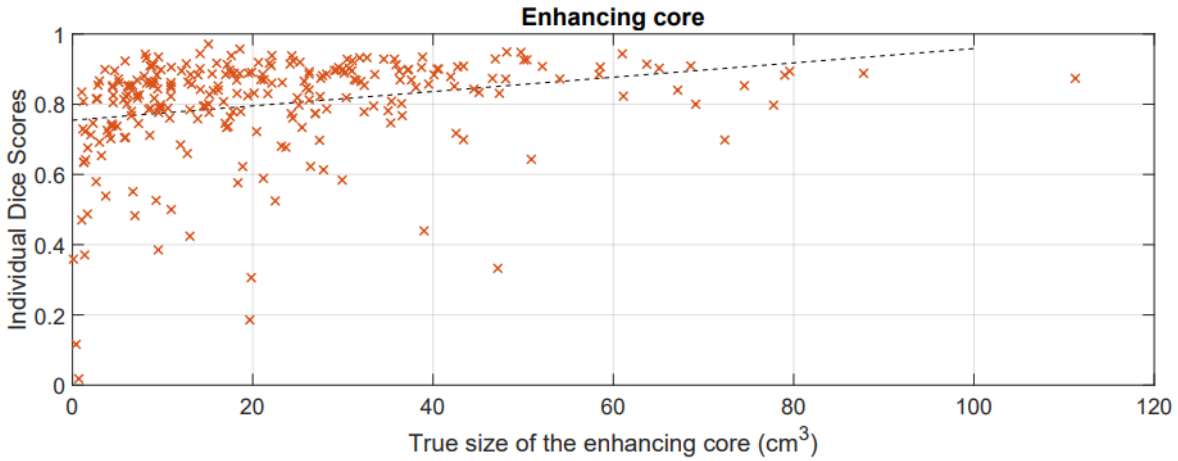

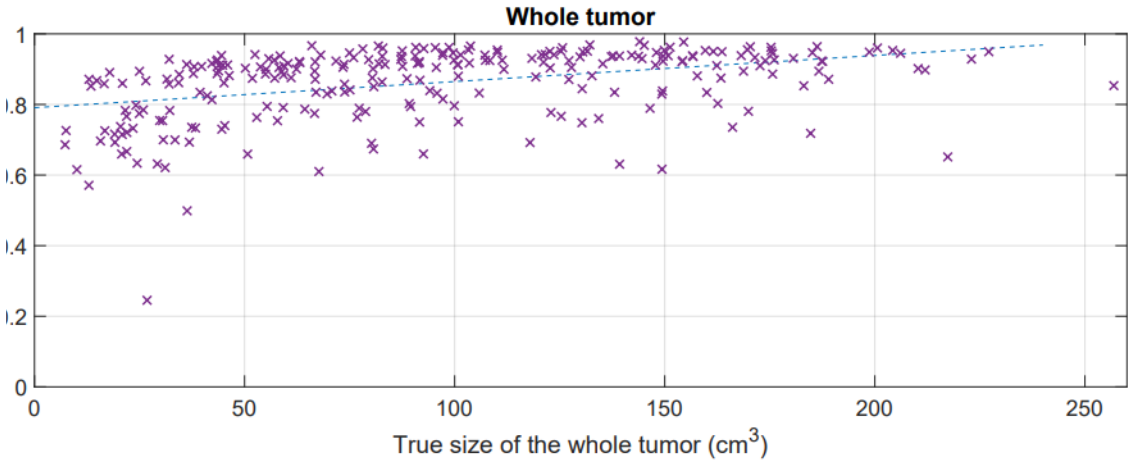

Comparison

Paper	Classifier	Data set	Test items	Average Dice score ED	EC	TC	WT
Csaholczi *et al.*[29]	random forest	BraTS15 train	220	0.6566	0.6728	0.6554	0.7722
Unpublished	XGBoost	BraTS19 train	259	0.7112	0.7895	0.7795	0.8339
Kamnitsas *et al.*[16]	CNN ensemble	BraTS15 train	274	N/A	0.728	0.754	0.901
Kamnitsas *et al.*[16]	CNN ensemble	BraTS15 test	110	N/A	0.634	0.667	0.849
Ding *et al.*[17]	ResNet	BraTS15 test	93	N/A	0.63	0.71	0.86
Bhalerao *et al.*[18]	3D Res U-net	BraTS19 test	125	N/A	0.697	0.772	0.828
Wang *et al.*[30]	3D U-net	BraTS19 test	125	N/A	0.778	0.798	0.852
Lefkovits *et al.*[31]	CNN ensemble	BraTS19 train	259	0.8005	0.7671	N/A	0.878
Proposed	U-net	BraTS19 train	259	0.7368	0.8005	0.7912	0.8612

Brain tissue segmentation with U-net

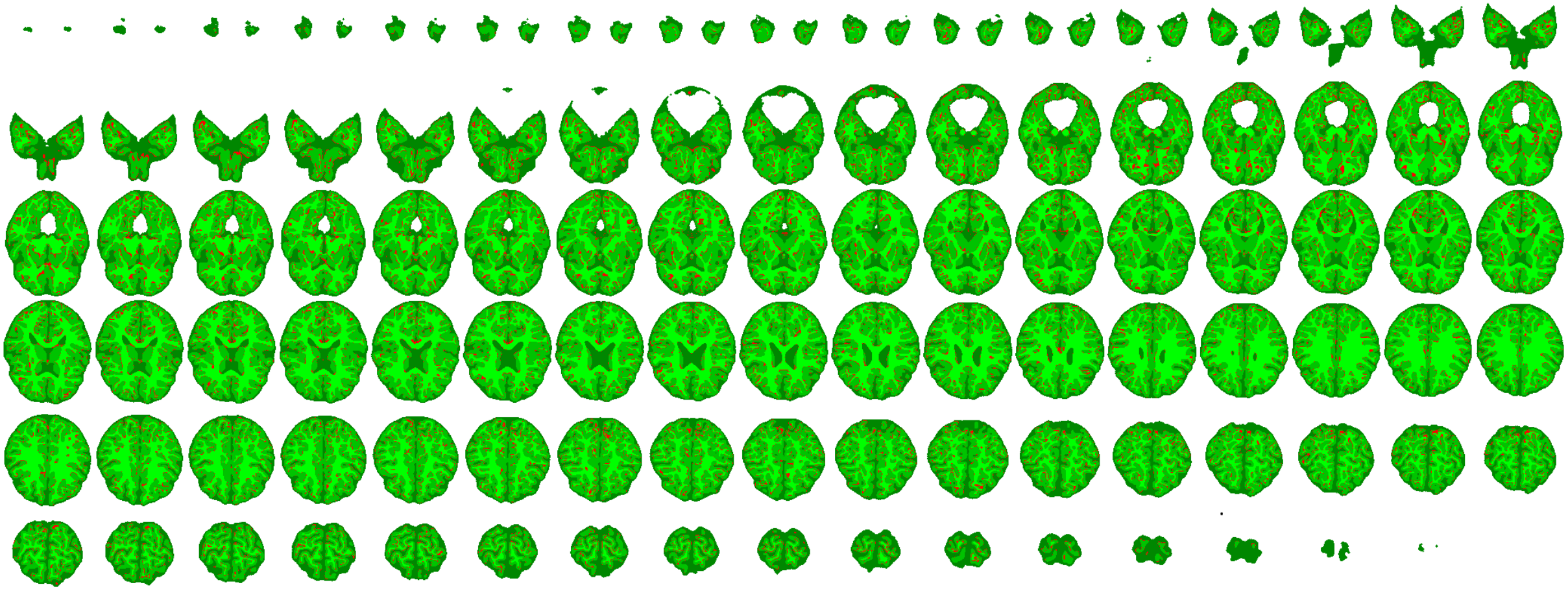

Input Data for Tumor Classification

Problem	Glioma	Meningioma	Pituitary	Positives	Negatives	Total
2-class [26]	-	-	-	1536	1500	3036
3-class [27]	1424	710	930	-	-	3064
4-class [28]	826	822	827	-	395	2870

[26] www.kaggle.com/datasets/ahmedhamada0/brain-tumor-detection, last visited on 14 December 2023.

[27] M. Nickparvar, "Brain Tumor MRI Dataset [Data set]," Kaggle, 2021, https://doi.org/10.34740/KAGGLE/DSV/2645886

[28] S. Bhuvaji, A. Kadam, P. Bhumkar, S. Dedge, and S. Kanchan, "Brain Tumor Classification (MRI) [Data set]," Kaggle, 2020, https://doi.org/10.34740/KAGGLE/DSV/1183165

Some network architectures

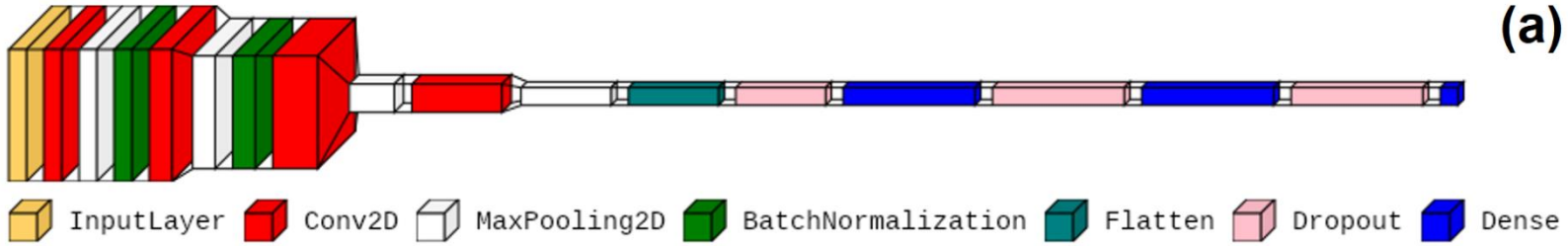

(a)

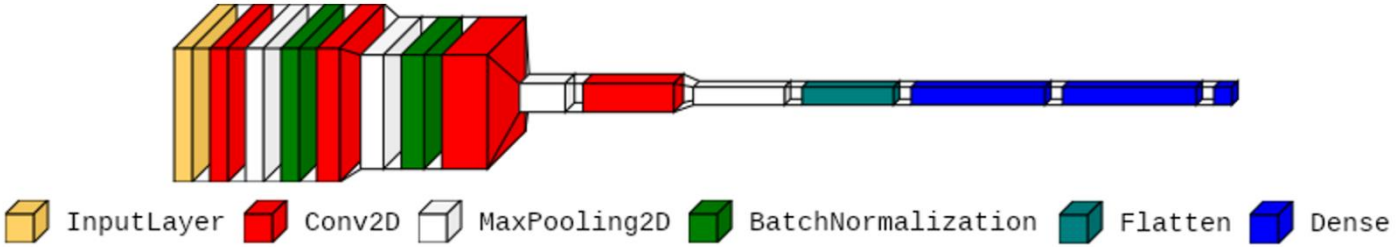

(b)

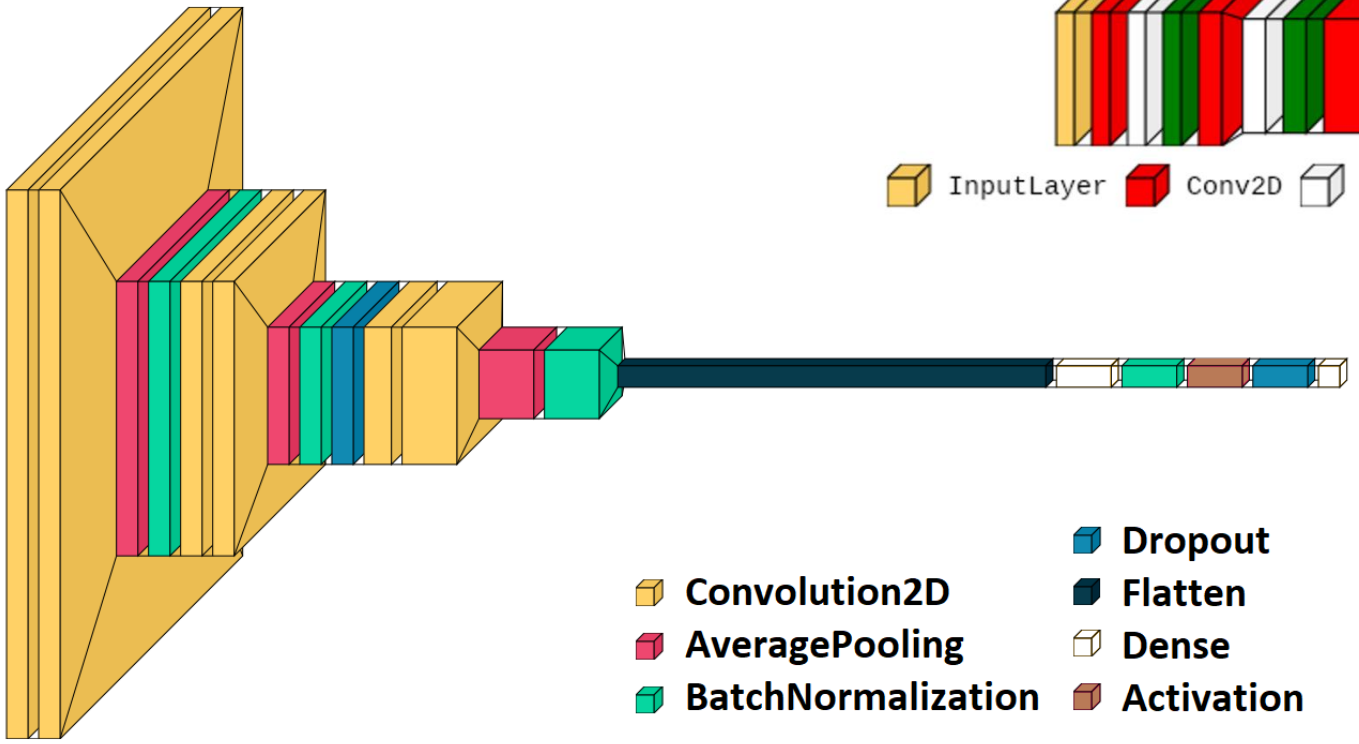

Results – 4 classes

	Glioma	Meningioma	Pituitary	Negative
Glioma	804	19	2	1
Meningioma	16	762	14	30
Pituitary	0	4	819	4
Negative	6	11	8	370
Recall	0.9734	0.9270	0.9903	0.9367
Precision	0.9734	0.9573	0.9715	0.9136
Dice score	0.9734	0.9419	0.9808	0.9250
Accuracy	0.9599			

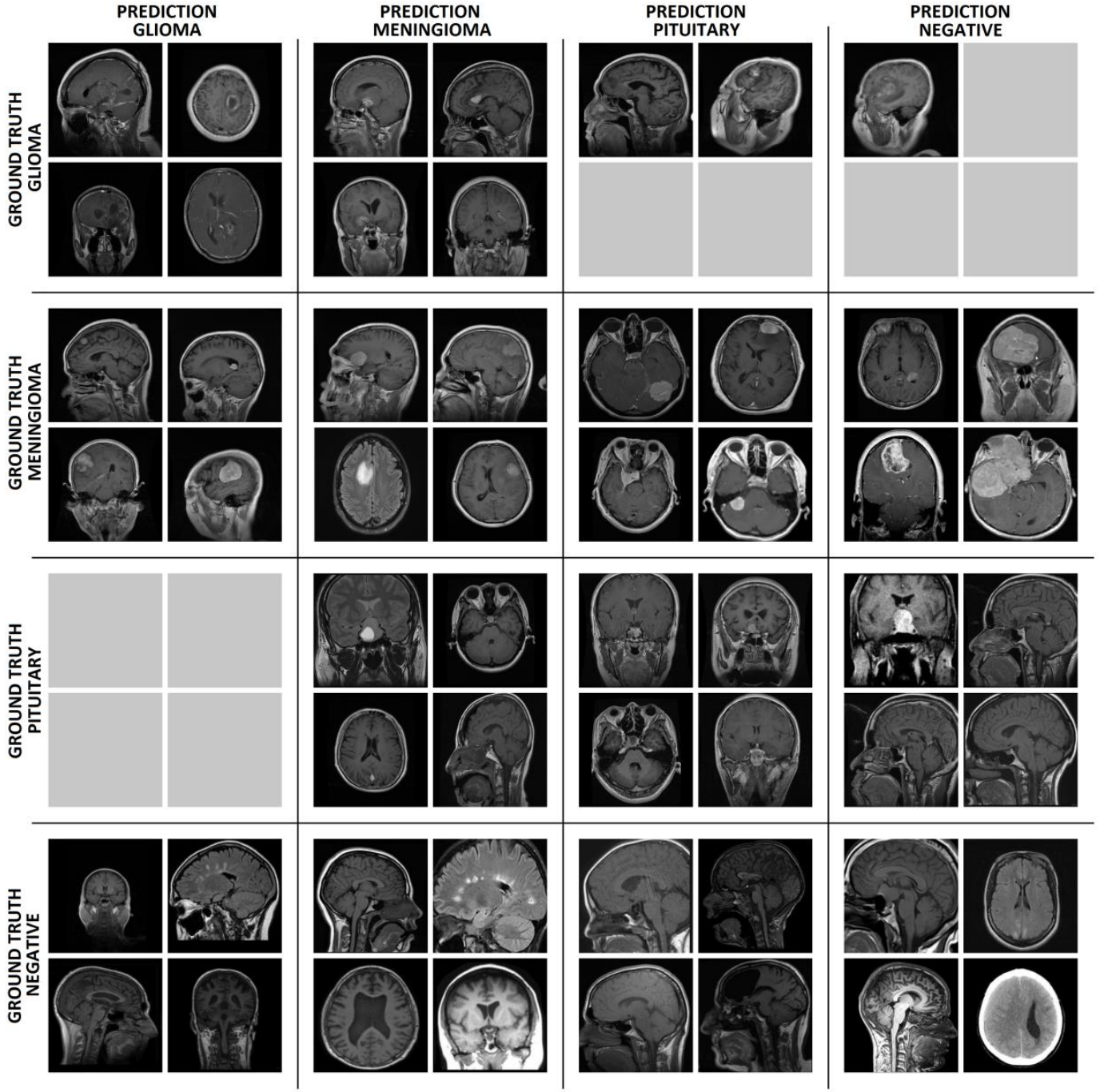

Results – 3 classes

	Glioma	Meningioma	Pituitary
Glioma	1402	19	3
Meningioma	34	672	4
Pituitary	0	1	929
Recall	0.9846	0.9465	0.9989
Precision	0.9763	0.9711	0.9925
Dice score	0.9804	0.9586	0.9957
Accuracy		0.9801	

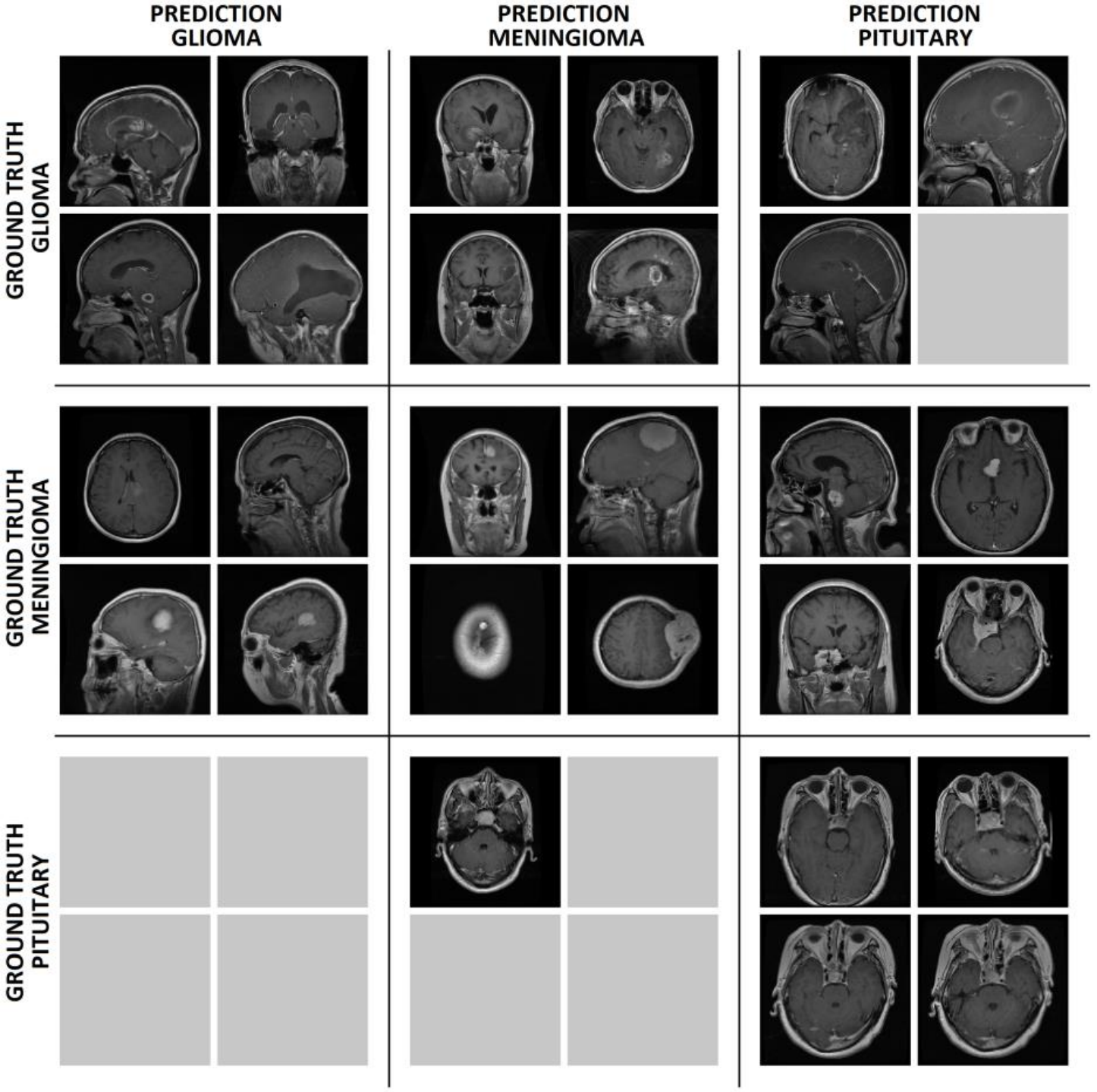

Results – 2 classes

ACCURACY BENCHMARKS OF THE 2-CLASS CLASSIFICATION PROBLEM

	Negative	Positive
Negative	1486	14
Positive	20	1516
Recall	0.9907	0.9870
Precision	0.9867	0.9908
Dice score	0.9887	0.9889
Accuracy	0.9888	

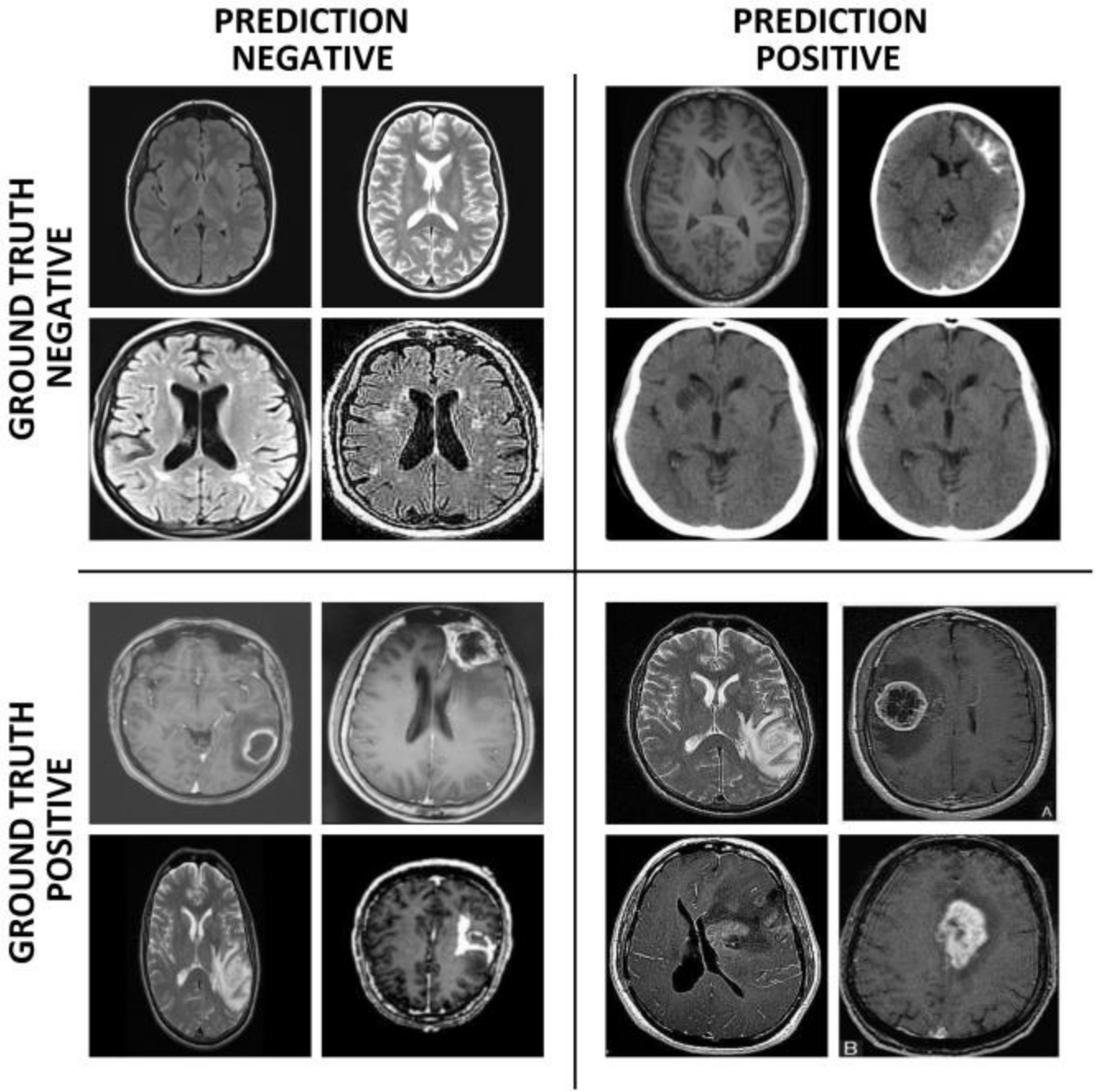

Other study: best performing models

Rank no.	CNN network	Dense neurons	Image size	Parame-ters	F1 score mean ± stdev	Accuracy mean ± stdev	AUC Meningioma mean ± stdev	AUC Glioma mean ± stdev	AUC Pituitary mean ± stdev
R1	⋆VGG	256	256 × 256	[MA][D]	0.9827 ± 0.0066	0.9827 ± 0.0066	0.9961 ± 0.0008	0.9981 ± 0.0013	0.9987 ± 0.0013
R2	⋆VGG	2048	256 × 256	[MA][D][K9]	0.9814 ± 0.0042	0.9814 ± 0.0042	0.9949 ± 0.0035	0.9973 ± 0.0023	0.9988 ± 0.0021
R3	⋆VGG	2048	256 × 256	[MA][K9]	0.9814 ± 0.0029	0.9814 ± 0.0030	0.9957 ± 0.0020	0.9975 ± 0.0019	0.9995 ± 0.0008
R4	⋆VGG	1024	256 × 256	[MA][D]	0.9808 ± 0.0037	0.9807 ± 0.0037	0.9967 ± 0.0010	0.9980 ± 0.0015	0.9988 ± 0.0011
R5	⋆VGG	1024	128 × 128	[MA][D]	0.9795 ± 0.0018	0.9794 ± 0.0019	0.9940 ± 0.0044	0.9967 ± 0.0022	0.9994 ± 0.0008
R6	⋆VGG	256	256 × 256	[MA]	0.9789 ± 0.0054	0.9788 ± 0.0056	0.9935 ± 0.0016	0.9968 ± 0.0016	0.9992 ± 0.0010
R7	⋆VGG	4096	256 × 256	[MA][D]	0.9782 ± 0.0053	0.9781 ± 0.0054	0.9942 ± 0.0024	0.9972 ± 0.0020	0.9981 ± 0.0020
R8	⋆VGG	2048	128 × 128	[MA][D][K9]	0.9781 ± 0.0037	0.9781 ± 0.0038	0.9941 ± 0.0043	0.9963 ± 0.0017	0.9975 ± 0.0023
R9	⋆VGG	32	128 × 128	[MA]	0.9778 ± 0.0047	0.9778 ± 0.0047	0.9943 ± 0.0018	0.9973 ± 0.0015	0.9991 ± 0.0009
R10	⋆VGG	4096	128 × 128	[MA][D]	0.9776 ± 0.0046	0.9775 ± 0.0047	0.9930 ± 0.0025	0.9958 ± 0.0015	0.9985 ± 0.0012

		Predicted			Predicted			Predicted			Predicted			Predicted		
	Class	Meningioma	Glioma	Pituitary	Meningioma	Glioma	Pituitary	Meningioma	Glioma	Pituitary	Meningioma	Glioma	Pituitary	Meningioma	Glioma	Pituitary
Actual	Meningioma	691	10	7	681	17	10	681	19	8	685	13	10	687	14	7
	Glioma	24	1399	3	25	1401	0	25	1401	0	29	1396	1	36	1390	0
	Pituitary	5	4	921	3	2	925	3	2	925	3	3	924	4	2	924
		Rank R1			Rank R2			Rank R3			Rank R4			Rank R5		
Actual	Meningioma	685	13	10	685	12	11	678	22	8	673	24	11	673	24	11
	Glioma	29	1396	1	34	1391	1	22	1401	3	28	1398	0	28	1398	0
	Pituitary	3	3	924	7	2	921	6	6	918	3	2	925	3	2	925
		Rank R6			Rank R7			Rank R8			Rank R9			Rank R10		

Comparison

Paper	Classif. method	Test images	Accuracy (test samples) 2-class	3-class	4-class
Toğaçar et al [20]	SVM	93	0.9677	–	–
Vankdothu et al [21]	RCNN	394	0.9517	–	–
Rajeev et al [22]	LSTM	978	0.9949	–	0.9834
Cheng et al [23]	SPM	3064	–	0.9128	–
Isunuri et al [24]	EfficientNet	1739	–	0.9835	–
Rahman et al [25]	Parallel DCNN	200+	–	0.9610	0.9560
Dénes-F. et al [19]	VGG	3064	–	0.9822	–
Proposed	CNN	2800+	0.9888	0.9801	0.9599

Conclusions

- Tumors of $10cm^3$ size can be easily detected
- Most tumors can be segmented with 85-90% Dice score, that is approx. 98.5% accuracy of pixelwise decisions
- CNN + DL are the current state-of-the-art
  - perform better
  - work longer, decisions hardly explainable

Some papers

- A. Győrfi, L. Szilágyi, L. Kovács: A Fully Automatic Procedure for Brain Tumor Segmentation from Multi-Spectral MRI Records Using Ensemble Learning and Atlas-Based Data Enhancement. Applied Sciences 11(2):564, 2021.
- A. Győrfi, L. Kovács, L. Szilágyi: A two-stage U-net approach to brain tumor segmentation from multi-spectral MRI records. Acta Universitatis Sapientiae – Informatica, 14(2):223–247, 2022.
- L. Dénes-Fazakas, G. Eigner, L. Kovács, L. Szilágyi: Two U-net Architectures for Infant Brain Tissue Segmentation from Multi-Spectral MRI Data. IFAC World Congress 2023, IFAC PapersOnLine 56(2):5637-5642, 2023.
- S. Csaholczi, L. Kovács, L. Szilágyi: Brain Tumor Classification Using Convolutional Neural Networks and Deep Learning. ICCC 2024, pp. 399-404.
- L. Szilágyi, Á. Győrfi, L. Dénes-Fazakas, S. Csaholczi, I.M. Pisak-Lukáts, L. Kovács: Challenges and Difficulties of Multi-Spectral MRI Based Brain Tumor Detection and Segmentation, ICHST 2023, pp. 1-6.
- A. Kőble, A. Győrfi, S. Csaholczi, B. Surányi, L. Dénes-Fazakas, L. Kovács, L. Szilágyi: Identifying the most suitable histogram normalization technique for machine learning based segmentation of multispectral brain MRI data. IEEE AFRICON 2021, pp. 71–76.
- A. Győrfi, S. Csaholczi, I.M. Pisak-Lukáts, L. Dénes-Fazakas, A. Kőble, O. Shvets, Gy. Eigner, L. Kovács,, L. Szilágyi: Effect of spectral resolution on the segmentation quality of magnetic resonance imaging data. INES 2022, pp. 53–58.

Team

- **PhD students**
  - **Lehel Dénes-Fazakas**
  - **Ágnes Győrfi**
  - **Szabolcs Csaholczi**
  - **Ioan M. Pisak-Lukáts**
- **Collaborators**
  - **László Lefkovits**
  - **Szidónia Lefkovits**
- **Special thanks**
  - **Levente Kovács**
  - **Vladik Kreinovich**